

Article

Arctic Inshore Biogeochemical Regime Influenced by Coastal Runoff and Glacial Melting (Case Study for the Templefjord, Spitsbergen)

Maria Pogojeva ^{1,2,*}, Alexander Polukhin ¹ , Petr Makkaveev ¹, André Staalstrøm ³, Anfisa Berezina ^{1,4}  and Evgeniy Yakushev ^{1,3,5,*} 

- ¹ Shirshov Institute of Oceanology, Russian Academy of Sciences, 117997 Moscow, Russia; aleanapol@gmail.com (A.P.); makkaveev55@mail.ru (P.M.); fisa4247@gmail.com (A.B.)
² N. N. Zubov's State Oceanographic Institute, Roshydromet, 119034 Moscow, Russia
³ Norwegian Institute for Water Research, 0579 Oslo, Norway; Andre.Staalstrom@niva.no
⁴ Institute of Earth Sciences, St. Petersburg State University, 199034 Saint Petersburg, Russia
⁵ V.I.Ilichov Pacific Oceanological Institute, Far Eastern Branch, Russian Academy of Sciences, 690041 Vladivostok, Russia
* Correspondence: pogojeva_maria@mail.ru (M.P.); evgeniy.yakushev@niva.no (E.Y.)

Abstract: Observations and predictions show that consequences of climate warming such as declining summer sea ice cover, melting glaciers, thawing permafrost, and increased river runoff to the Arctic Ocean will likely modify processes relevant to the freshwater and carbon budget, which in turn affect high-latitude marine ecosystems. There is a knowledge gap in terms of understanding the seasonal variability of biogeochemical characteristics in coastal environments, first of all due to a lack of winter data. More data are also needed on the biogeochemical composition of different environmental media, i.e., sediments, snow, and ice. The aim of this work was to assess the current biogeochemical regime of a fjord system exposed to coastal runoff and glacial melting and discuss the possible consequences connected with climate warming. We used data from five expeditions to the Templefjord, West Spitsbergen, obtained in different seasons (February 2011, September 2011, March 2014, June 2015, and June 2017). In all the expeditions, the distributions of dissolved oxygen, nutrients, and carbonate system parameters in the water column were studied. The principal environmental media, i.e., seawater, bottom sediments, river water, sea ice, river ice, glacier ice, and snow, were sampled. The collected data allowed us to describe seasonal dynamics in the water column and to estimate the concentrations of the parameters under study in different environmental media. Our observations revealed the glacial and river footprints in the water column biogeochemistry; the glacial influence can be traced both in summer and in winter season. The results demonstrated the significant influence of coastal runoff and melted glacier water on the carbonate system and nutrient regime in the Templefjord, and can be extrapolated to other Arctic fjord systems.

Keywords: biogeochemical regime; Arctic Ocean; glaciers; coastal runoff; nutrients; acidification; Spitsbergen



Citation: Pogojeva, M.; Polukhin, A.; Makkaveev, P.; Staalstrøm, A.; Berezina, A.; Yakushev, E. Arctic Inshore Biogeochemical Regime Influenced by Coastal Runoff and Glacial Melting (Case Study for the Templefjord, Spitsbergen). *Geosciences* **2022**, *12*, 44. <https://doi.org/10.3390/geosciences12010044>

Academic Editors: Yongwei Sheng and Jesus Martinez-Frias

Received: 12 October 2021

Accepted: 4 January 2022

Published: 17 January 2022

Publisher's Note: MDPI stays neutral with regard to jurisdictional claims in published maps and institutional affiliations.



Copyright: © 2022 by the authors. Licensee MDPI, Basel, Switzerland. This article is an open access article distributed under the terms and conditions of the Creative Commons Attribution (CC BY) license (<https://creativecommons.org/licenses/by/4.0/>).

1. Introduction

Impacts of climate change have already been reported in the Arctic Ocean (AO) [1–3]; examples are increased temperature [4], decreasing sea-ice extent [5], freshening [6], increase in Arctic rivers discharge [7], and increasing surface carbon dioxide concentrations, with concomitant ocean acidification [8]. Observations and predictions show that declining summer sea ice cover and increased river runoff to the Arctic Ocean will lead to changes in the freshwater and carbon budget, which in turn affect the high-latitude marine ecosystem. Compared with the 1980–2000 average, the volume of freshwater in the upper layer of the Arctic Ocean has increased by 8000 cubic km (more than 11%) [9]. The increase in

atmospheric CO₂ and elevated oceanic CO₂ uptake, with the consequences of decreased pH and carbonate ion concentrations, are expected to put further stress on marine organisms, in particular calcifiers [10]. The largest ocean acidification signal (pH decline) in the world's oceans is expected in relatively cold and fresh Arctic surface waters [8,11,12]. In addition to the direct effects—changes in pH and carbonate ion concentrations in marine organisms and ecosystems—indirect links could also occur, through changes in biogeochemical cycling of substances, especially nutrients and their bioavailability for primary production [13].

The Arctic coastal water, in addition to the processes occurring in seawater, is subject to processes occurring on the land, i.e., glaciers melting, coastal abrasion, and permafrost thawing influence riverine and coastal discharge water quantity and quality. This is well evidenced in a series of works [14–16] dedicated to carbonate chemistry dynamics in the Arctic Ocean as well as permafrost thawing's influence on coastal water properties [16–19].

Glaciers cover many Arctic islands and, in particular, about 60% of the Svalbard archipelago [20]. Nowadays, many of them are retreating and have shown decreasing glacier volume (e.g., [21–23]), increasing in turn the freshwater supply to the nearby fjord and ocean. One of the consequences of “atlantification” is a longer ice-free period in the Svalbard area in the recent decades, primarily due to a contemporary increase in the temperature of inflowing waters [24]. In Svalbard, the inflowing warm Atlantic water has the potential to melt the glacier fronts at the tidewater glaciers of West Svalbard [25]. In studies by Fransson et al. [25], it was shown that increased freshwater supply with glacial drainage water decreased carbonate saturation state, pH, and alkalinity. The stratification of Svalbard coastal water is generally due to seasonal warming of the surface layer and fresh water supply from melting glaciers, river runoff sustained by land-terminating glacial meltwater, and snow melt [26]. The deep and subsurface waters of the fjords are subject to advection of Atlantic waters, largely driven by local wind conditions entering the fjord from the shelf [27].

Generally, biogeochemical processes in the Arctic coastal environments and their connection with climate change are understudied, making it difficult to assess the potential impacts. There is a knowledge gap in terms of understanding the seasonal variability of biogeochemical characteristics in the coastal environment, first of all due to a lack of winter data. Moreover, more data are needed on the content of biogeochemical characteristics in different environmental media, i.e., sediments, snow, and ice.

The aim of this work was to assess the current biogeochemical regime of a fjord system in Svalbard exposed to coastal runoff and glacial melting, depicting the seasonal variability in the fjord as well as the contrast between its glacier-influenced and outer areas. To assess the current biogeochemical regime in the fjord, we need to evaluate its main seasonal features. It is also necessary to learn how coastal discharge and glacial melting affect biogeochemical properties and what parameters can be better used for detecting riverine and glacial water. It is important to estimate concentrations in the main environmental media, i.e., seawater, bottom sediment, river water, sea ice, river ice, and glacier ice, to evaluate the rates of transformation of elements in coastal environments.

We performed our studies in Templefjord, Spitzbergen, Norway, hosting a glacier and a river, and carried out measurements in different seasons. For this we used a unique infrastructure available in Longyearbyen and performed our studies on winter and summer expeditions [28,29].

2. Materials and Methods

2.1. Study Area

Templefjord is located in the inner part of Isfjord on the west coast of Spitsbergen island, which is part of Svalbard archipelago, neighboring the Arctic Ocean, the Norwegian Sea, and the Greenland Sea. At the head of this 14-km-long fjord, there is a calving tidewater glacier named Tunabreen and two land-terminating glaciers, von Postbreen and Bogebreen, running into the Templefjord. The drainage area of Tunabreen glacier is approximately 190 km² and it is now retreating from its maximum extent in 2004 [30]. The fjord is relatively

shallow in the inner part. The depth is 50 m near the glacier and 110 m in the main basin (central and outer fjord) [25]. A small river, the Murdochhelva, flows into the northern coast of the fjord approximately 8 km from the Tunabreen glacier. This river is basically a stream draining from Murdochbreen glacier, located 4–5 km from the coast. The geographical position of the fjord allows the inflow of warm and saline Atlantic water by the West Spitsbergen Current [26]. A distinct sill is absent in Templefjord [31], allowing the free exchange of water with the open ocean. A surface water mass with large seasonal and interannual variability and an intermediate mass of shelf water mixed with advected waters from the Atlantic can be distinguished [25].

In this study a total of five expeditions were performed in different seasons from 2011 to 2017 (Table A8). Two were conducted in the winter (February 2011 and March 2014) and three in the summer (September 2011, June 2015, and June 2017). The positions of sampling stations are shown in Figure 1.

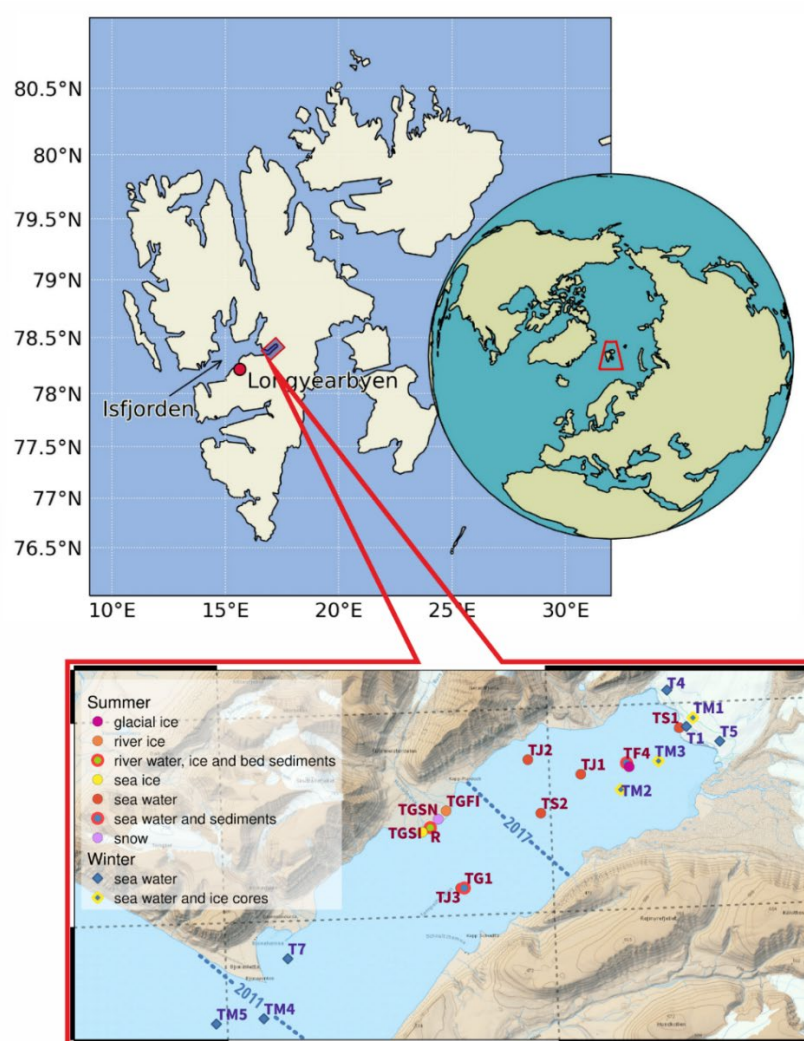


Figure 1. Positions of the stations sampled in the expeditions in February 2011 (T1, T4, T5, T7), September 2011 (TS1, TS2), March 2014 (TM1, TM2, TM3, TM4, TM5), June 2015 (TJ1, TJ2, TJ3), and June 2017 (TG1). The stations in the fjord mouth (TM4 and TM5) were taken in the winter from a boat when it was impossible to sample in the central part of the fjord due to ice conditions. The dotted lines indicate the winter positions of the solid ice boundaries in 2017 and 2011.

During the winter expeditions, the fjord was covered with ice. In 2011, the solid ice boundary was in the fjord mouth, allowing sampling from the ice at all stations. In 2017, solid ice was found only in the inner part of the fjord; stations TM1–TM4 were

sampled from the ice and station TM5 from the boat, since the outer fjord was clogged with drifting ice.

River water was sampled at Station R in 2015 and 2017.

The expeditions were based in Longyearbyen and the sampling sites were accessed by snowmobiles in the ice-covered part of the fjord and by boats in the open part depending on the season. The first day analyses were performed at the laboratory of the University Centre in Spitzbergen, Longyearbyen (UNIS).

2.2. Methods and Data

The samples were collected from typical Arctic media: seawater, river water, sea bottom sediments, river bottom sediments, sea ice, river ice, glacier ice, and snow. Samples of seawater were collected during all expeditions (under the ice in February 2011 and March 2014), and samples of river water during the summer expeditions. Sea ice was sampled in March 2014 (at Stations TM1, TM2, and TM3; Figures 1 and A4, Table A1) and June 2017 (St. R, and near St. TJ1 from a drifting iceberg, Table A4). In 2017, the bottom sediments (collected at St. TG1, TF4, TG8, R) and different types of ice (collected near St. R, and near St. TJ1 from drifting pieces of ice) were studied. Bottom sediments were collected with a grab in 2017 at St. TG1, TF4, TG8, R (Figure A10, Tables A2, A3 and A5).

The following parameters were determined in the collected water samples: temperature, salinity, dissolved oxygen, pH, total alkalinity (Alk), phosphate (PO_4), sum of nitrate and nitrite (NO_x), silicate (SiO_2), total dissolved inorganic carbon (TIC), and dissolved organic carbon (DOC). The list of parameters studied varied in different expeditions (see Table A8).

For the water column, we used a CTD profiler Sea Bird SBE 911 (Bellevue, [WA], USA), or SAIV A7S (Laksevag, Norway) that measured temperature and conductivity/salinity, and a 1 L HydroBios (Altenholz, Germany) bottle for water sampling. Depending on the vertical structure, they were sampled at from 2 to 5 depths. Water samples for dissolved oxygen were collected in 50-mL calibrated flasks and titrated following the Winkler method in the few hours after sampling. Samples for the determination of pH were collected in 100-mL plastic bottles without preservation. Nutrients were sampled into 100-mL plastic bottles and preserved with sulfuric acid (1 mL of 4N H_2SO_4) [32]. Samples for Alk and TIC were collected in 500-mL borate bottles and fixed with 0.250 mL of concentrated HgCl_2 . Samples for DOC were collected in dark glass 100-mL bottles and preserved with 1 mL of 4N sulfuric acid according to accredited Norwegian procedures [32].

Ice cores were sampled in March 2014. The temperature was measured with a digital thermometer along the ice core with discreteness of 10 cm. The cores were transported to the lab in polyethylene bags. In the lab, they were divided into 10-cm layers (three layers from 30-cm-thick ice) and melted in light conditions in a room at 5 °C for approximately 12 h. The same analyses were conducted in melted ice water samples as in the other water samples.

For the bottom sediment sampling, we used a grab. The samples from the 0–5-cm upper layer were packed into plastic bags and delivered frozen to the lab. From the extracted liquid, using centrifugation sediment porewater, we measured the content of alkalinity, total inorganic carbon, phosphate, nitrate, and silicate. Samples from an abrasive cliff were collected in plastic bags that were frozen and further processed in a similar way as the bottom sediment samples.

First day analyses were carried out at the laboratory of UNIS (Longyearbyen); other samples were preserved and sent to the laboratories of NIVA (the Norwegian Institute for Water Research), IO RAS (the Shirshov Institute of Oceanology, Russian Academy of Sciences) and SOI (N. N. Zubov's State Oceanographic Institute, Roshydromet) for further analyses.

Oxygen, nutrients, and DOC were determined by the procedures of [32,33]. Samples for dissolved oxygen in water were titrated within a few hours after sampling using the Winkler technique. Samples for pH were thermostated (25 °C) and measured also in the

few hours after collecting. During the various expeditions, pH measurements were taken by the traditional potentiometric pH technique (pH-P) and with the spectrophotometric technique (pH-S) recommended for ocean acidification studies [34]. pH-P was measured with a pH meter Metrohm 780, (Giessen, Germany), with the electrode calibrated before every measurement. We performed pH-S measurements with a 5-cm cell-equipped HACH DR-2800 (Colorado, USA) field spectrophotometer that measured the absorbance at three wavelengths simultaneously after the addition of m-cresol purple dye to the sample in a 1:100 ratio according to [34]. More details are given in [35]. pH-P and pH-S operate with different pH scales: the NBS (NIST, IUPAC) scale for pH-P and total scale for pH-S. The total scale defines pH in terms of the sum of the concentrations of free hydrogen ion and HSO_4^- . The difference in pH values between these scales is about 0.13 [36]. A similar difference (0.146) was observed in field studies in the Barents Sea (about 100 measurements; our data). In this study, the results were presented using the NBS scale, which is applicable to both seawater and freshwater. Data from the expedition in 2011, when only spectrophotometric pH was applied, were transformed into NBS scale using the difference of 0.14. Nutrients were measured spectrophotometrically at the NIVA lab following accredited Norwegian procedures [37]; phosphates were measured using techniques by Murphy and Riley, dissolved silica was measured according to the method of Koroleff, and ammonia was analyzed with phenol-hypochlorite Sagi–Solorzano method. The technique of nitrate nitrogen determination was based on the reduction of nitrates to nitrites and subsequent colorimetry.

Alk and TIC samples collected in all the expeditions were measured in the lab with a VINDTA system [38] using Certified Reference Materials (CRM, purchased from A. Dickson, Scripps Institution of Oceanography, USA), with the resultant accuracy in the order of the precision. The components of the carbonate system were calculated according to [33] using the CO2SYS program [39]. During the calculations we used pH, Alk, phosphate, silicic acid, salinity, temperature, and depth (pressure) as input. The calculations were made using the NBS scale for pH, the H_2SO_4 dissociation constant of Dickson, solubility products of aragonite and calcite of Mucci, and the carbonic acid dissociation constants (K_1 and K_2) of Mehrbach, as refitted by Dickson and Millero. Concentrations of carbonate ions (CO_3^{2-}), bicarbonate ions (HCO_3^{2-}), total dissolved inorganic carbon (TIC), carbon dioxide partial pressure ($p\text{CO}_2$), and aragonite saturation (Ω_{ar}) were calculated for the laboratory temperature conditions.

3. Results

3.1. Distribution of Hydrophysical and Biogeochemical Properties in the Water Column

3.1.1. Winter

During the winter expedition of 2011 (19 February 2011), we found no visible vertical gradients in the distribution of hydrophysical parameters; the water column was not stratified, and there was also no horizontal difference from the station near the glacier to the outer fjord (Figure 2). The distributions of temperature and salinity were homogenous, with values varying in the ranges 1.8–1.9 °C and 33.6–34.5 psu from surface layer to the bottom near the glacier and in the outer fjord. No significant concentration changes were observed for the biogeochemical parameters. They were distributed homogeneously with values of about 350 μM for O_2 , 8.33 NBS for pH, 0.55 μM for PO_4 , 7 μM for NO_x , 5–10 μM for SiO_2 , 2330–2360 $\mu\text{mol/kg}$ for Alk, and 2140–2170 $\mu\text{mol/kg}$ for TIC (Figure 2). The calculated $p\text{CO}_2$ was about 400 μatm and the calculated aragonite saturation was 1.35. A single exception is an increase of SiO_2 to 10 μM below the ice, observed only at station near the glacier, St. T1, but not at St. T4 (Figure A1) and T5 (Figure A2) sampled nearby.

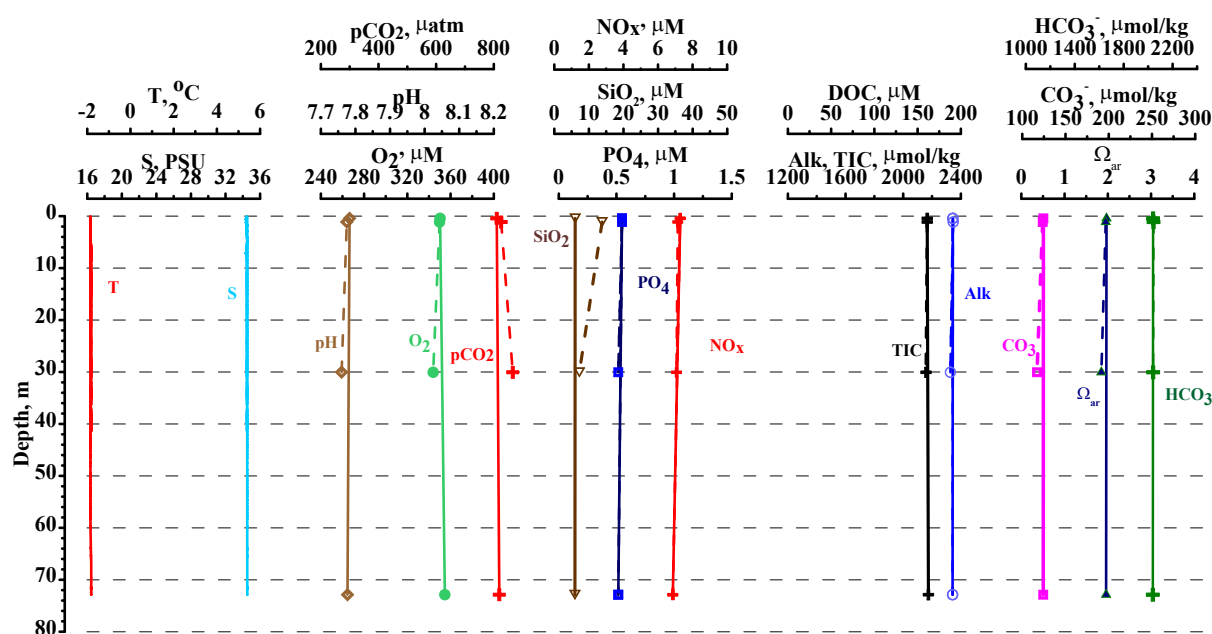


Figure 2. Vertical distribution of the temperature, T, salinity, S, pH, pH, dissolved oxygen, O_2 , phosphate, PO_4 , nitrate, NO_x , silicate, SiO_2 , dissolved organic carbon, DOC, total alkalinity, Alk, total inorganic carbon, TIC, carbonate, CO_3 , partial pressure of CO_2 , pCO_2 , and aragonite saturation (Arag. Sat.) at the station near the glacier T1 (dotted line) near the outlet T7 (solid line), sampled on 19 February 2011.

A similar vertically uniform distribution was observed in March 2014 near the fjord opening (St. TM4, TM5, in Figures 3, A5 and A6), but the distributions near the glacier were different (St. TM3 in Figure 3 and St. TM1 in Appendix A.1.2, Figure A3). Here, a strong vertical salinity gradient was detected 1 m below the ice, where the salinity dropped from 34.8–34.9 psu in the deeper layer to 27 psu near the ice. The temperature changed from -1.75 °C in the deep layers to -1.5 °C just below the ice.

The nutrient concentration in the surface layer under the ice cover was higher than in 2011: 0.8 – 1.0 μM for PO_4 , 9 – 10 μM for NO_x and 10 – 25 μM for SiO_2 . Alk and TIC showed a slight decrease beneath the ice (to 2339 $\mu mol/kg$ and 2200 $\mu mol/kg$, respectively) in comparison with the deeper layer. The high concentration of dissolved oxygen (355 – 390 μM), high pH (8.21 – 8.43 NBS), and low pCO_2 (200 – 300 μatm) indicate the beginning of phytoplankton development directly under the ice. The ice cores collected in these stations had a brown color in the lower parts, showing the presence of algae in the ice.

On site TM5 (14 km away from the solid ice and 1.5 km from pancake ice), no freshening in the surface water was detected. The entire water column at the site was well mixed, with salinity at about 35 psu. The temperature rose slightly, from -1.5 °C on top to -1 °C near the bottom. O_2 had the lowest value in the surface layer (328 μM). Nutrient concentrations increased slightly from the surface to the bottom layer; however, the water structure was generally homogenous.

Strong maxima of 52 μM and 24 μM were detected at 44 m depth at St. TM3 (Figure 3) and under the ice at St. TM1 (Appendix A.1.2, Figure A3). In the same sample from 44 m at St. TM3 (Figure 3), the concentration of phosphate was 1.98 μM , which is twice the maximum concentration measured during our studies (about 1 μM).

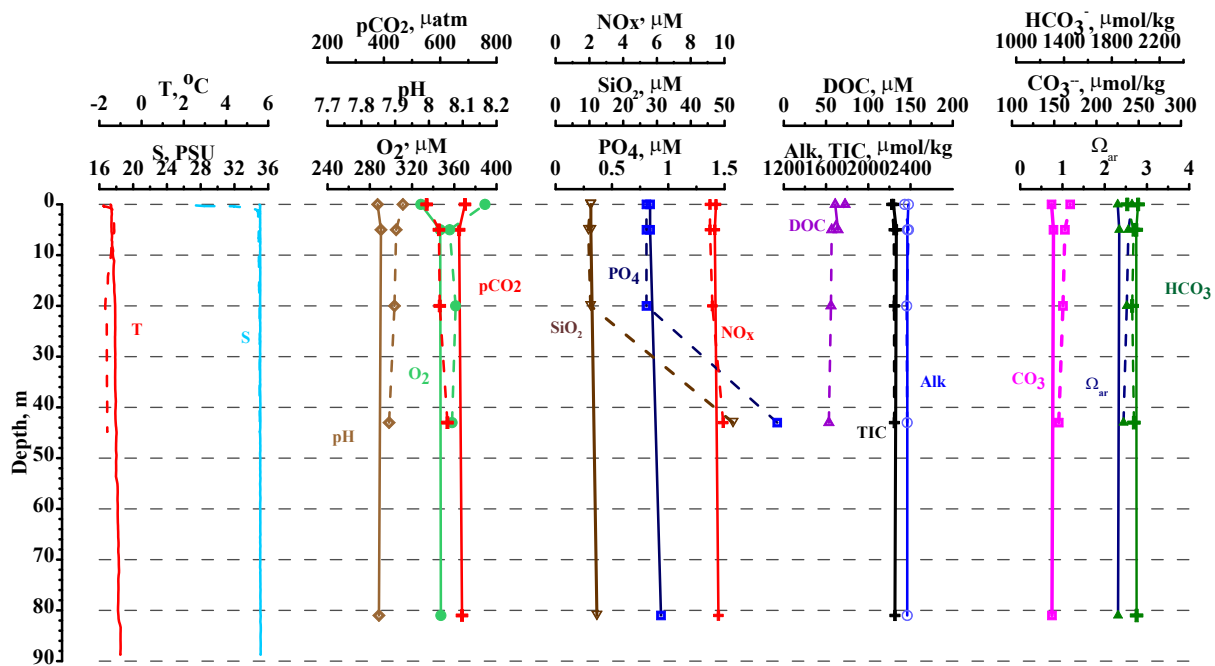


Figure 3. Vertical distribution of physical and chemical parameters at stations TM3, near the glacier (dotted line), and TM5, in the fjord outlet (solid line), sampled on 19 March 2014.

Alk near the glacier slightly decreased from 2378 $\mu\text{mol/kg}$ to 2339–2345 $\mu\text{mol/kg}$, and TIC from 2238 $\mu\text{mol/kg}$ to 2200–2222 $\mu\text{mol/kg}$. We detected an increase in pH from 8.21 to 8.21–8.40 near the glacier, and an increase in aragonite saturation from 1.65 to 1.78–1.89.

3.1.2. Summer

The summer period was characterized by a well-developed water column stratification. A thin (<1 m) surface water layer with low salinity was detected in the June expeditions (Figures 4 and A7). Below the thin surface layer, there was a layer where the salinity slightly increased to about 20 m. This 20-m upper thermocline layer was characterized by changes in temperature: it decreased from 2.77 $^{\circ}\text{C}$ near the surface to -0.90 $^{\circ}\text{C}$ at 20 m depth.

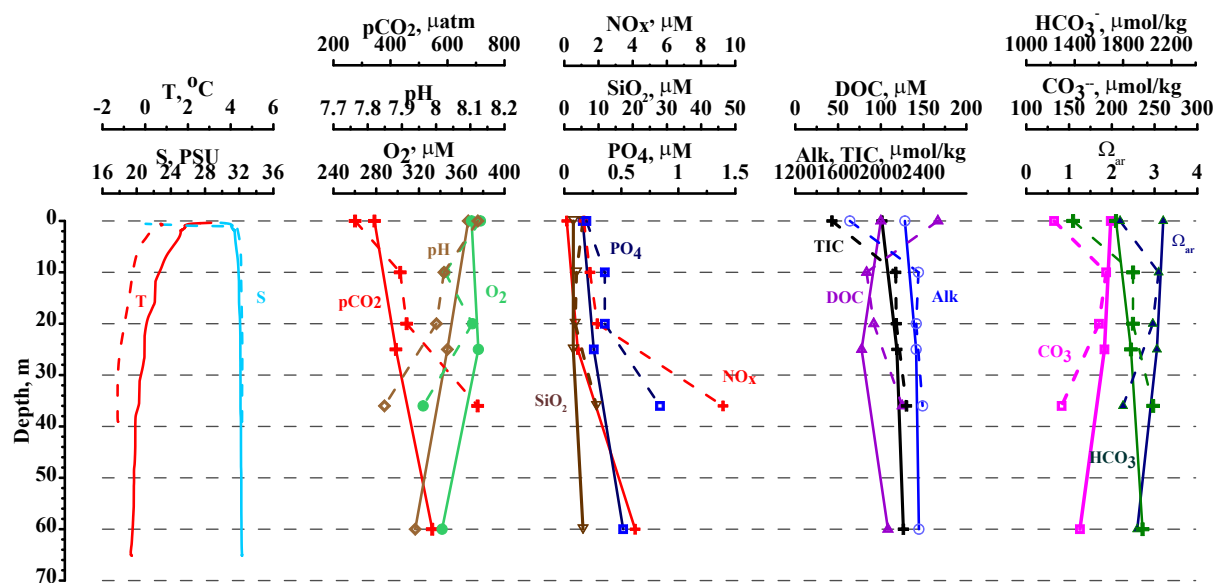


Figure 4. Vertical distribution of physical and chemical parameters at stations TJ1 near the glacier (dotted line) and TJ3 in the middle of the fjord (solid line), sampled on 17 June 2015.

A clear hydrophysical stratification affected the distribution of all the studied biogeochemical parameters in June. Compared to the deeper water, the upper 20 m layer was characterized by higher values of O₂ (334–377 μM) and pH (8.32–8.41) and lower values of PO₄ (0.19–0.36 μM), NO_x (1.1–1.9 μM), and SiO₂ (3.2–3.6 μM) (Figure 4).

In the surface layer, a difference in the carbonate system parameters could be detected between a station near the glacier (St. TJ1) and one in the middle of the fjord (St. TJ3). Surface layer pCO₂ increased from 276 μatm to 343 μatm and Ω_{ar} increased from 2.19 to 3.20 from the glacier and halfway out in the fjord. The highest value of Ω_{ar} was detected at 60 m at Station TJ3 (2.81), which is comparable to the highest values of Ω_{ar} in the open Arctic Ocean [40].

In September, this upper low saline layer was smoothed, and salinity gradually increased in a 10-m layer (Figure 5). This layer was characterized by higher temperatures, fluctuating between 3 and 4 °C, probably due to various wind conditions prior to sampling. At station TS1 close to the Tunabreen glacier in September, the average salinity over the surface layer (0–2 m) was 21.1 psu, and at station TS2 (in the middle of the fjord) it was 27.1 psu. Below 10 m, it was uniformly distributed with values of 32.7–33.2 psu. At the surface, the water oxygen concentration changed from 366.2 μM at Station TS1 near the glacier to 333.6 μM at St. TS2. Therefore, an increased freshwater supply of glacial drainage water could be detected in the salinity profile and oxygen distributions.

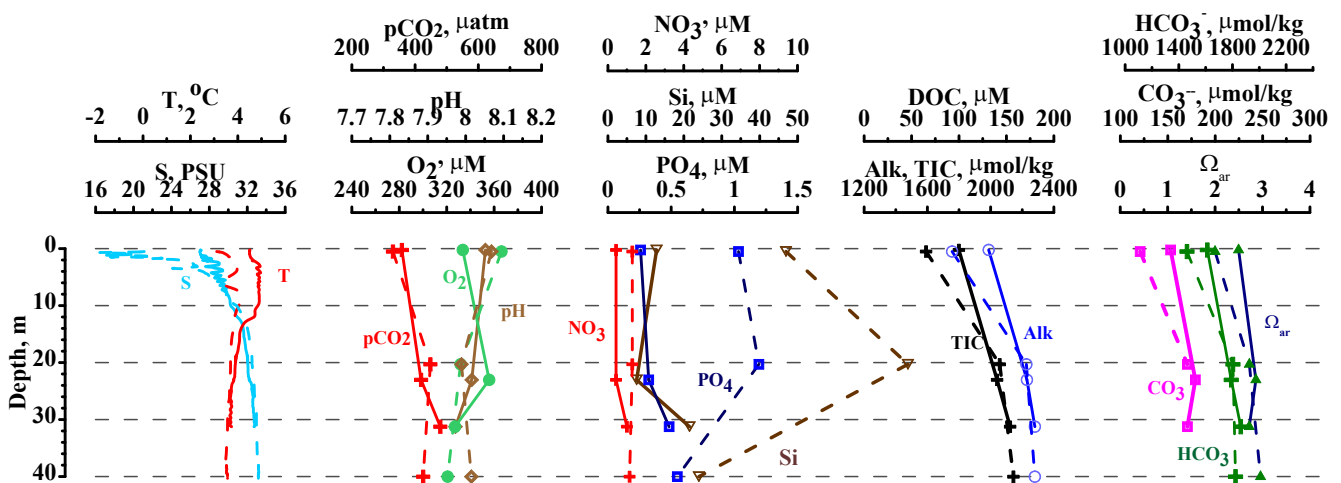


Figure 5. Vertical distribution of physical and chemical parameters at stations TS1 near the glacier (dotted line) and TS2 in the fjord outlet (solid line), sampled on 06 September 2011.

A small river, the Murdochelva, flowing out from the northern coast of the fjord, formed a plume spreading from the river’s mouth to the surrounding water. This plume was detected as a thin (several decimeters) layer in June 2017 at St. TG1 (Figure 6), located in the middle of the fjord, about 2 km from the coast and 8 km from the glacier. At this station, the surface water had increased values of PO₄ (1.5 μM), NO_x (about 4 μM), and an extremely high value of SiO₂ (59 μM), much higher than the background values (0.25 μM, 0.15 μM, and 2 μM, correspondingly). The plume water was characterized by a decrease in Alk (from 2.3 μmol/kg to 1.2 μmol/kg) and TIC (from 2.0 μmol/kg to 1.2 μmol/kg) compared to the deeper water.

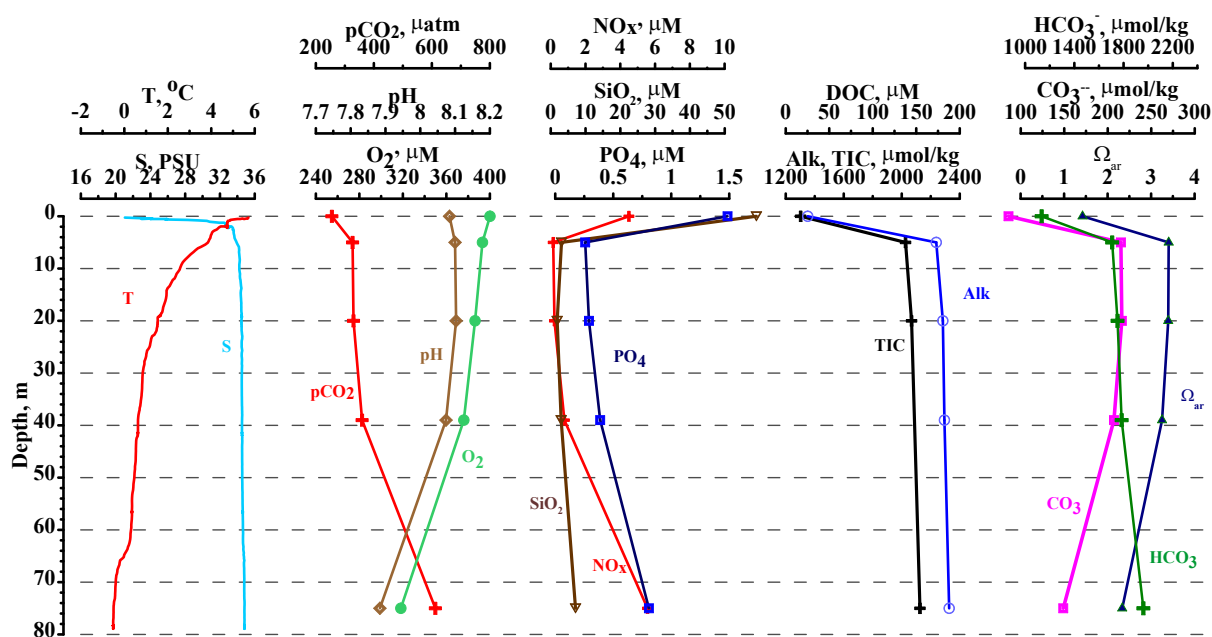


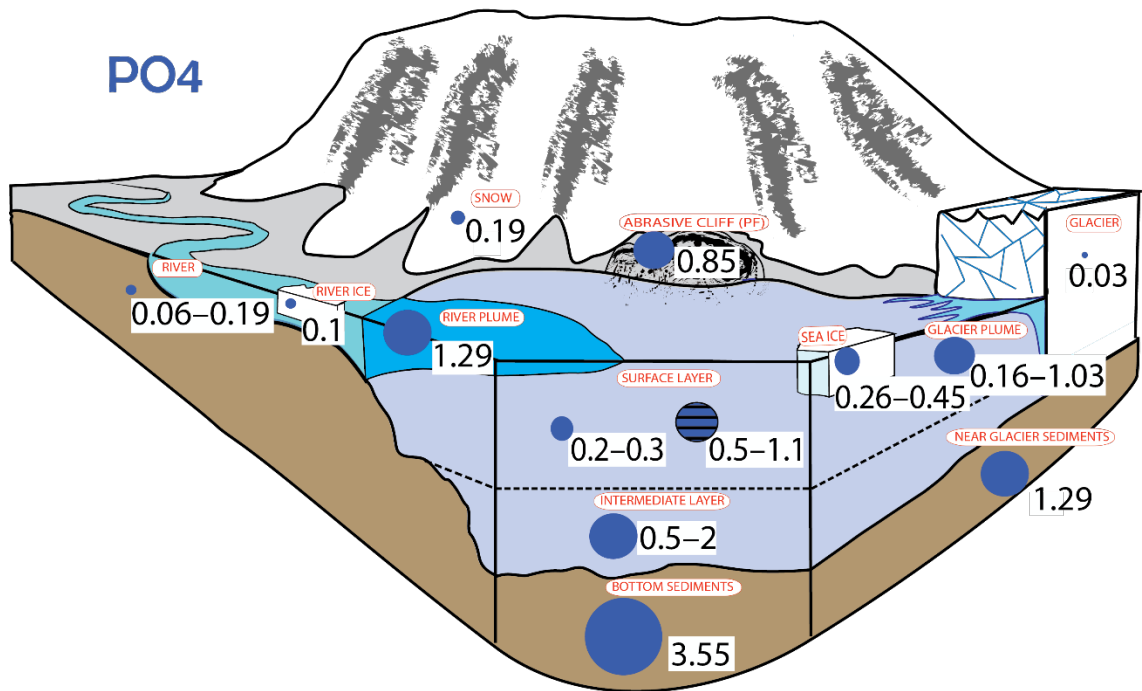
Figure 6. Vertical distribution of physical and chemical parameters at station TG1 (12 June 2017).

3.2. Comparison of Nutrient Concentrations in Different Arctic Media

The data collected in different environmental media are summarized in Figures 7 and 8. They demonstrate the relative content of nutrients in the environmental media of a coastal system, i.e., seawater, river water, snow, sea ice, river ice, glacial ice, permafrost from an abrasive cliff, sea sediments near the glacier, and sea sediments in the outer fjord. For the seawater we saw concentrations in the surface layer in the outer fjord, in the surface layer near the glacier influenced by the glacial plume, in the river plume, and in the intermediate layer. We also observed seasonal variability of the nutrients in the surface layer of seawater.

As follows from Figures 7 and 8, for phosphate, silicate, and nitrate the lowest concentrations were observed in the ice (glacial ice was the lowest)—0.03 μM , 1.3 μM , and 0.2 μM , respectively. The highest were in the sediments: 3.6 μM , 239 μM , and 17.1 μM . Concentrations in the material from abrasive cliff (permafrost) were smaller than those in the sediments and comparable to the concentrations in seawater. The hierarchy of concentrations for phosphate and silicate was similar, but for nitrate some differences could be noticed. First of all, the concentrations of nitrate in the surface water were higher in the hierarchy pyramid, suggesting the limitation by nitrogen in these waters. The second important difference was that the concentration of nitrate in marine sediments was significantly lower in the outer fjord than near the glacier—the opposite situation to phosphate and silicate. During the sampling, the color of the sediments in the outer fjord was black (indicating reduced conditions), and near the glacier red-yellow (indicating oxic conditions). We can hypothesize that the sediment in the outer fjord is enriched with organic matter compared with the sediment near the glacier that opened to exchange with the water column after the last Tunabreen glacier surge event in 2004 [41]. Mineralization of organic matter requires oxygen, and when oxygen is depleted, denitrification starts and nitrate is consumed [42,43]. That is why we observed very low concentrations of nitrate in the sediment in the outer fjord, and high concentrations of nitrate near the glacier where oxygen was not depleted, because of small concentrations of organic matter that did not accumulate here after the last glacier surge in 2004.

(A)



(B)

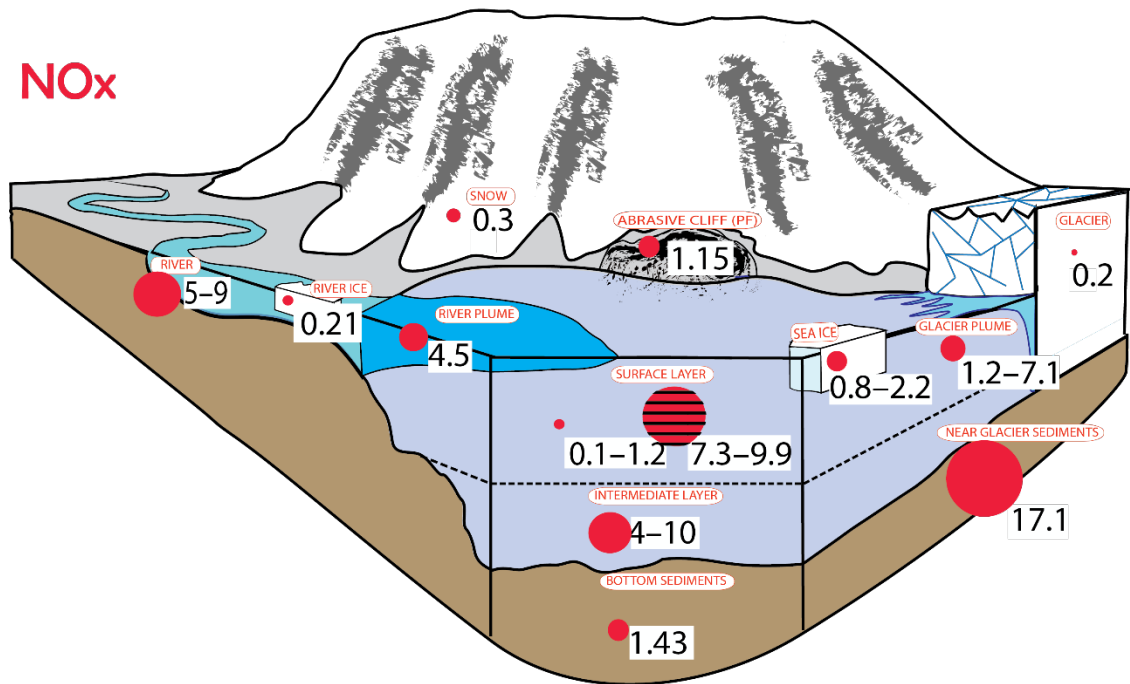


Figure 7. Cont.

(C)

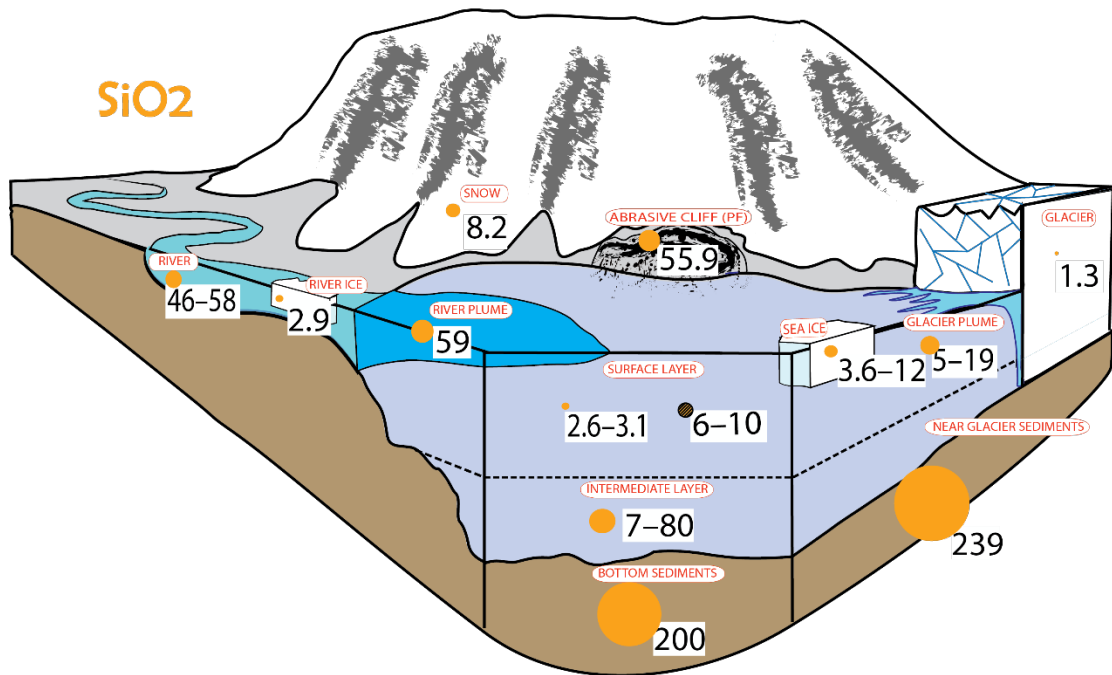


Figure 7. Content of phosphate (A), silicate (B), and nitrate (C) in the following environmental media: seawater, bottom sediment, river water, sea ice, river ice, glacier ice, snow, and abrasive cliff (permafrost). For the seawater, we saw concentrations in the surface layer in the outer fjord, in the surface layer near the glacier influenced by the glacial plume, in the river plume, and in the intermediate layer. Concentrations or ranges of concentrations are given in μM . Circles show relative change of concentrations; the dashed circle corresponds to the winter (only in the surface water).

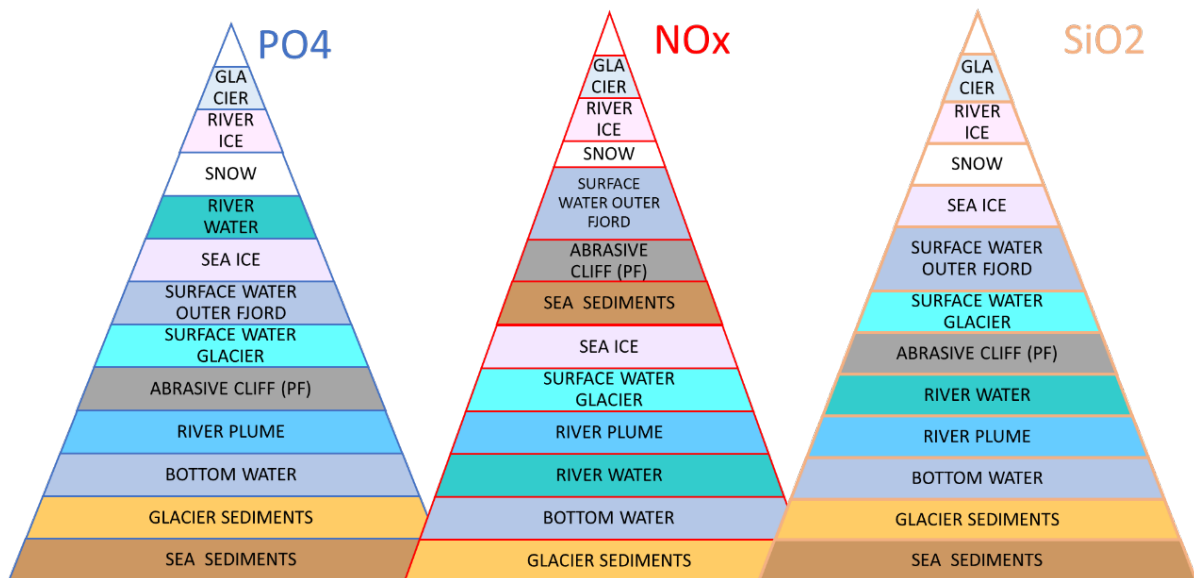


Figure 8. Hierarchical change of concentrations of phosphate, nitrate, and silicate in the following environmental media: seawater, bottom sediments, river water, sea ice, river ice, glacier ice, and snow.

4. Discussion

4.1. Seasonality

When considering the reasons for the seasonal variability of the biogeochemical characteristics: in the fjord system, we can name the following key factors affecting the

seasonal variability of the biogeochemical characteristics: formation and destruction of stratification, continental runoff, and aquatic biota activity. The first and main factor is the formation of density stratification in the summer and its destruction in winter, which affects the distributions of all hydrophysical, chemical, and biological properties. The stratification is generally due to seasonal warming of the surface layer and fresh water supply from melting glaciers, river runoff sustained by land-terminating glacial meltwater, and snow melt [26]. The deep and subsurface waters of the fjords are subject to the advection of Atlantic waters, which is largely driven by wind that enters the fjord from the shelf [27]. The second factor is coastal runoff. According to [27], two coastal runoff periods can be distinguished in June, with dominating discharge of the melting water from the snow, and in July with dominating glacial melt water. The third factor that affects the seasonality is the processes of production and destruction of organic matter—first of all, an intensive phytoplankton bloom typically occurring in Svalbard in May [27].

Investigation of the seasonal changes of biogeochemical regime in the High Arctic is connected with the logistical challenges of taking measurements; these studies, especially in the winter, are very scarce. Our observations represent the results of several 1–2-day expeditions performed in different seasons in the six-year interval from 2011 to 2017; of course, the problem of the comparability of data collected in the same month in different years arises. The changes we observed can be connected with seasonal variability and with the interannual variability connected with climate change, which has led to remarkable environmental changes in the Arctic.

As an example, the interannual variability of the thermohaline properties was studied by [44], who noted that the water temperature in the Templefjord depends on an influx of seawater from the open ocean. They found that, in 2010, the water temperature 10 km from the glacier varied from $-1.8\text{ }^{\circ}\text{C}$ to $-1.1\text{ }^{\circ}\text{C}$, which is higher than the water temperature of $-1.9\text{ }^{\circ}\text{C}$ measured near Tunabreen. However, in 2011, the water temperature 10 km from the glacier varied from $-1.86\text{ }^{\circ}\text{C}$ to $-1.82\text{ }^{\circ}\text{C}$ and was almost the same as near Tunabreen. Heat fluxes from the water column, which can have its origin outside the fjord, can also significantly reduce the ice thickness 10 km from Tunabreen [44].

These interannual changes in hydrophysical properties could also affect the hydrochemical data discussed here. On top of changes in the circulation patterns responsible for the fjord water flushing, there might be changes in temperature, precipitation, and other factors. Nevertheless, the data we received allow to demonstrate that the seasonal signal dominates over the interannual changes, and we see that the data collected in the same months or season in different years are comparable to a greater degree than the data from different seasons in one year.

As follows from Figures 2–6, the seasonal variability of the biogeochemical parameters is well pronounced in the surface layer. In Figure 9 (and Tables A6 and A7), we summarize data from different expeditions and show the variability of the concentrations of biogeochemical parameters in Templefjord through the year. We also show typical time periods of phytoplankton bloom, freshet, and glacial melting in relation to the dates of our studies. The variability at stations close to the glacier (T1, T4, T5, TS1, TM1, TM2, TM3, TJ1, TJ2, and TF4; see Figure 1) and stations in the outer fjord (T7, TS2, TM4, TM5, TJ3, and TG1) is given separately.

The measured concentrations of characteristics collected in the same season are close to each other, suggesting that the seasonal variability dominates over interannual changes.

To summarize, there are increases in the concentrations of dissolved oxygen and pH values in the summer compared with the winter, and a decrease in nutrients, phosphate, and nitrate in the summer compared with the winter that can be connected with the seasonality of the processes of synthesis and decay of organic matter. The maximum O_2 and pH and minimum nutrients were observed in June, while in September O_2 and pH values were lower and nutrient values slightly increased (Figure 9).

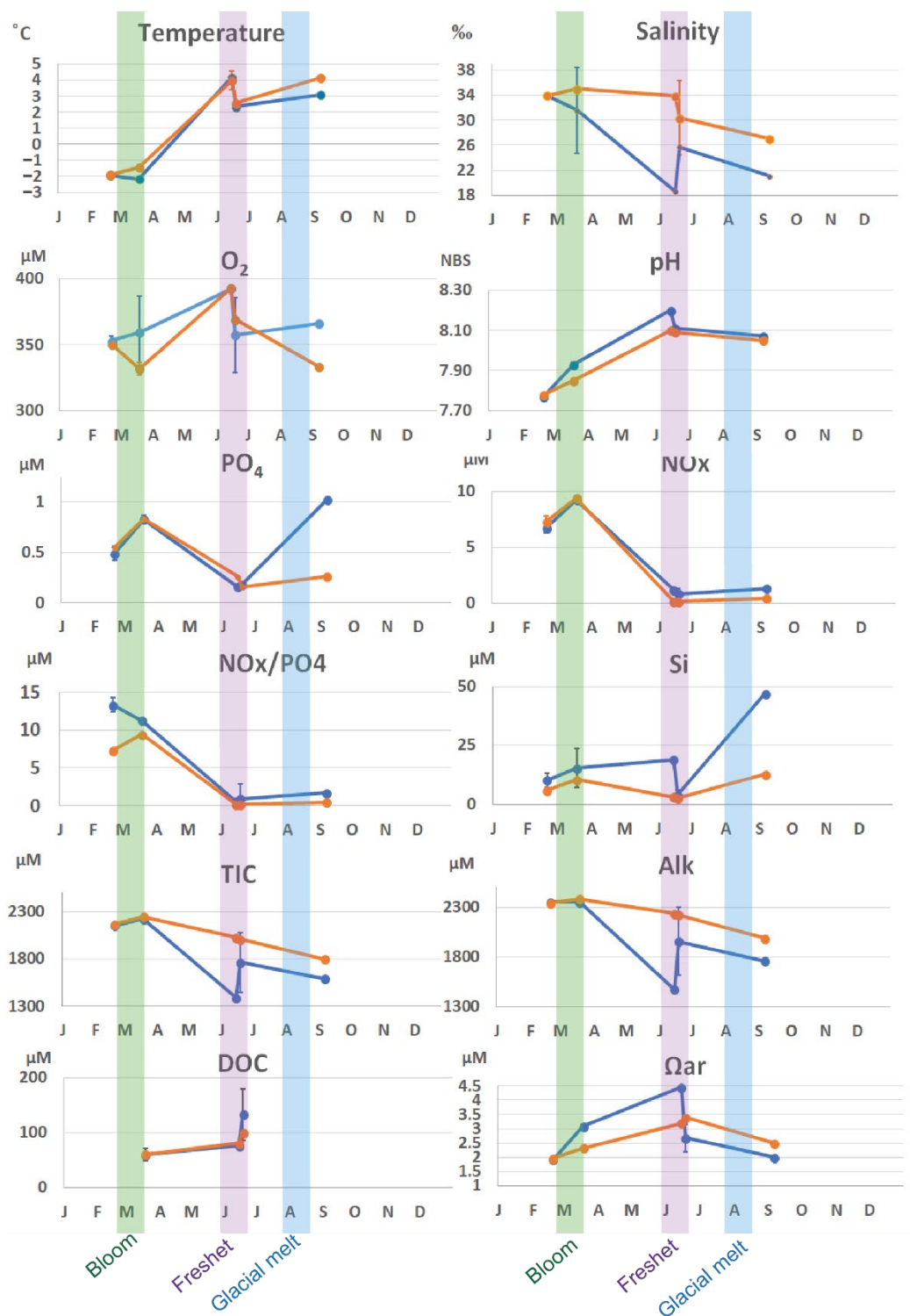


Figure 9. Seasonal variability of concentrations of biogeochemical parameters in the surface layer near the glacier (blue dots and blue line) and in outer Templefjord (orange dots and orange line) detected from February to September (horizontal scale) on expeditions in 2011–2017 (dots correspond to sampling time). Thick colored vertical lines show the typical periods of the spring bloom (green), freshet (pink), and glacial melt (blue). Thin vertical lines outline standard errors.

The seasonal variability in the quantity and quality of organic carbon and nutrients in Isfjorden [27] was explained by an intensive phytoplankton bloom in May, spring freshet in

June, and glacial meltwater in August. The same factors could also influence the changes in the marine surface waters seen in the current study.

In general, registered concentrations of inorganic nitrogen and phosphorus species in this study are close to other observations from Svalbard (Kongsfjorden), i.e., 6–11 μM for nitrogen and 0.8 μM for phosphorus [45,46].

Nutrient concentrations measured in the river water were close to those described in [27], while observations of DOC concentration in the Murdochelva were much lower—19.2 μM compared with the cited paper. According to [27], the concentration of DOC in rivers in June ranged from 670 to 1410 μM in the majority, with minimum values for Adventelva (40 μM). However, they observed higher values in Adventelva in May (980 μM). It can be assumed that the concentration of DOC in the Murdochelva was also higher in May, before our observations. The difference in the surface layer in our study and in [27] was not as high—196 μM and 91.6 μM , respectively.

4.2. Near Glacier vs. Outer Fjord

The data summarized in Figure 9 also show the difference in biogeochemical characteristics in the near-glacial region and the outer fjord in different seasons of the year, as per data collected on different expeditions from February to September.

The seasonal variability of temperature pointed to small differences near the glacier and in the outer fjord, but the variability of salinity differed significantly. There were similar values observed in February, but from March to September the near-glacier salinity was lower at about 5 psu, with a maximum difference of 15 psu detected in June. This graph clearly shows the freshening of the near-glacial waters.

In February, there was practically no difference in the concentrations of all the investigated biogeochemical parameters, which generally coincides with the studies performed in Templefjord in April 2013 [25]. A single exception is the high concentration of silicate measured near the glacier (Figure 3), which indicates the presence of glacial water discharge in winter even when there are no significant salinity minima. These sudden increases in SiO_2 concentrations could be marked out in different seasons at different depths (St. TS1 in Figure 5 in September; TF4 in Figure A9 in June). The high concentrations of SiO_2 detected in some samples are associated with glacial meltwater from contact with silica-rich bedrock [25]. The patchy distribution of SiO_2 can be explained by the nonuniformity of the glacial plume in the vicinity of the glacier. An upwelling of subglacial discharge is a known feature of the tidal fjords in Svalbard and Greenland [47,48], which could explain the observed increases in silicate at different depths near the glacier. In some cases, we observed a correlated enrichment of these samples with phosphate.

Our observations on the changes of the ice color and chemical composition under the ice near the glacier in March 2014 (St. TM3, Figure 3) indicate the development of the winter bloom in the ice and water fed by the subglacial discharge, which can be an important factor of the fjord's biogeochemistry in different regions [49].

In all the other seasons, from March to September, the water masses affected by the glacier could be clearly detected by a decrease in the concentrations of Alk and TIC. Concentrations of phosphate and nitrate showed no clear difference between the glacier-affected and fjord outlet waters during the photosynthetic period, but one can see an increase in their concentrations near the glacier in September, after the main bloom.

Dissolved oxygen (392.4 μM) and pH (8.46) maxima near the glacier in the June 2017 expedition were connected with photosynthesis intensification due to the nitrate increase near the glacier, which illustrates the influence of the glacial plume on the productivity of the fjord waters [50]. Evidently, nitrate is a limiting nutrient in these waters; the N:P ratio is less than the classical Redfield N:P = 16 throughout the year and drops to less than 2.5 in June and September (Figures 9 and 10). The N:P ratio near the glacier is generally higher due to the relative nitrate increase there.

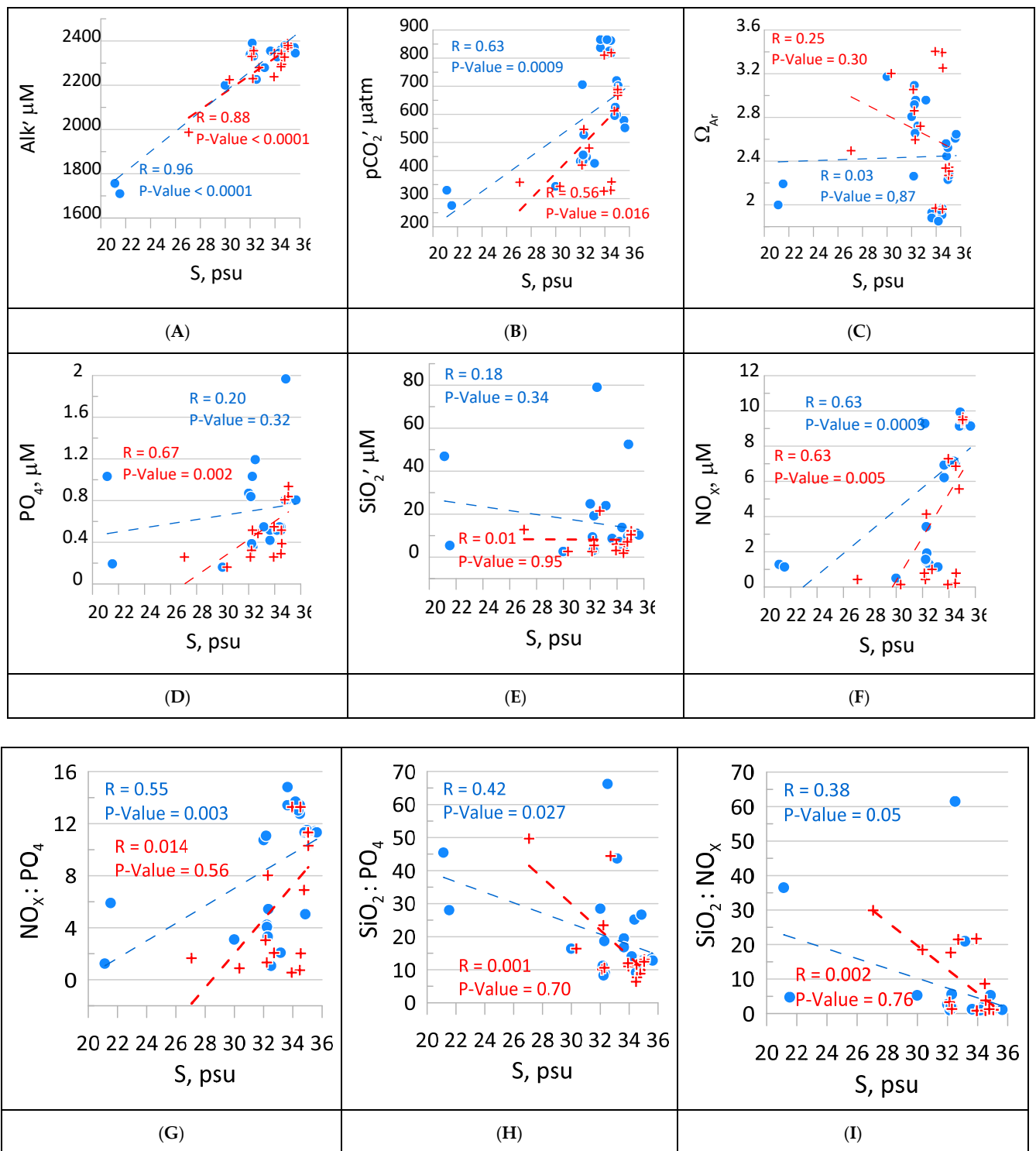


Figure 10. Distributions of Alk (A), pCO₂ (B), Ω_{Ar} (C), PO₄ (D), SiO₂ (E), NO_x (F), NO_x:PO₄ (G), SiO₂:PO₄ (H), and SiO₂:NO_x (I) versus Salinity(S) for the outer fjord (in red) and near the glacier (in blue). Fit linear lines, correlation coefficients R, and P-values are shown in red for the outer fjord and in blue for the near-glacier region.

DOC, measured in March 2014 and June 2017, showed similar values near the glacier and in the outer fjord, while in June 2015, DOC near the glacier was 1.3 times higher (133.3 μM vs. 100 μM). This DOC increase near the glacier could be connected with the

autochthonous organic matter that remained after the relatively more intensive bloom near the glacier.

In June, water near the glacial was characterized by very low Alk (1710 $\mu\text{mol}/\text{kg}$ in 2014 and 1956 ± 346 $\mu\text{mol}/\text{kg}$ in 2017) (Figure 9); this value was, however, even higher than that found by [25] in the Templefjord alkalinity in April and May 2012 (1142 $\mu\text{mol}/\text{kg}$), and in September (526 $\mu\text{mol}/\text{kg}$). On the contrary, we found silicate concentrations (15.3 ± 8.2 μM in June and 47 μM in September) much higher than those found by Fransson et al. [25] (less than 9 μM). This can be explained by the patchy nature of the silicate distribution near the glacier, which is potentially connected with the complex structure of the glacial plume.

In September, the nutrients and carbonate system parameters showed a clear spatial change along the surface waters of the fjord, demonstrating the influence of glacial waters (Figures 5 and 9). The surface layer Alk decreased from the glacier to the central fjord, from 1756 $\mu\text{mol}/\text{kg}$ (TS1) to 1988 $\mu\text{mol}/\text{kg}$ (Appendix A.1.4, Figure A8), while TIC increased from 1635 $\mu\text{mol}/\text{kg}$ to 1828 $\mu\text{mol}/\text{kg}$ and HCO_3^- from 1531 $\mu\text{mol}/\text{kg}$ to 1700 $\mu\text{mol}/\text{kg}$. The PO_4 , NO_x , and SiO_2 concentrations decreased from the inner to the outer part of the fjord, from 1.03 μM to 0.26 μM , from 1.29 μM to 0.43 μM , and from 46.93 μM to 12.82 μM , respectively. pCO_2 and Ω_{ar} increased from 195 to 230 μatm and from 1.40 to 1.77 from the glacier to the outer part of the fjord. Below 10 m, the distributions of the properties became practically uniform.

In Figure 10, we show the differences in the ratios of selected parameters to salinity in samples collected near the glacier (in blue) and in the outer fjord (in red). These two groups combine as surface water with seasonally decreasing salinity and intermediate water with high salinity throughout the year. As is demonstrated, there is a very good correlation between a conservative parameter Alk and salinity near the glacier as well as in the outer fjord waters. This corresponds to the connection between alkalinity and freshwater fraction in the Kongesfjorden described in [40]. However, for pCO_2 and Ω_{ar} , the correlation with salinity is poor, which is explained by the influence of organic matter production and destruction processes, which change through the year. It can be noted that, near the glacier, there were observed maximum values of pCO_2 and minimum values of Ω_{ar} . In the plots for PO_4 and SiO_2 , high concentrations near the glacier were found in low and high salinity, which can be explained by the detectability of the glacial origin water in the surface and in the deep. Phosphate and silicate were poorly correlated with salinity, while a better correlation was shown for NO_x ; the ranges of its changes were similar near the glacier and in the outer fjord.

In our studies, we did not detect a glacial plume as a water mass with a specific thermohaline and chemical properties, but we clearly see its influence, first of all in sporadic increases of phosphate and silicate concentrations. These sporadic increases can be clearly seen in the plots of $\text{SiO}_2:\text{PO}_4$ and $\text{SiO}_2:\text{NO}_x$ (Figure 10). Generally, this supports the finding of [49] that the glacial plume fuels productivity near the glacier. In all our observations, the $\text{NO}_x:\text{PO}_4$ ratio was less than 16, again indicating nitrate limitation, including near the glacier.

The total surface runoff from the Svalbard glaciers due to the melting of snow and ice is estimated at roughly 25 ± 5 $\text{km}^3\text{yr}^{-1}$ [51]. The greater part of this volume will come from glacial freshwater runoff as the frontal ablation decreases before the sea ice return in midwinter [52]. This surface water mass, which originated from the Svalbard glaciers' runoff, should have biogeochemical characteristics differing from those in the outer fjord and the open sea, as shown and discussed here.

4.3. River Plume

During our studies, we had only one sample illustrating the influence of a river plume on distributions at a station in the center of the fjord (Figure 6). This plume can be detected not only by a decreased value of salinity and alkalinity (1351 $\mu\text{mol}/\text{kg}$), as is common,

but also by very high concentrations of silicate (59.5 μM), close to those observed in rivers (47.5–57.5 μM).

The concentrations measured during the expedition in the river Murdochelva (St. R) were 0.19 μM for PO_4 , 5.07 μM for NO_x , 45.92 μM for SiO_2 , and 19.15 μM for DOC. Such a high concentration of nutrients in water of glacier origin could occur in a case of leaching of salt from the bedrocks, forming Spitzbergen mountains and shores [25]. This effect was experimentally demonstrated at the Novaya Zemlya in 2013 [53]. Meanwhile, the content of DOC in the riverine water during the observation period was low in comparison with the typical values for Svalbard rivers [27].

We demonstrate here that the river plume brought water with higher nutrient content compared with the nutrient background values in the surface seawater. It is known that, in other regions of the world, river plumes affect the biological productivity of coastal zones [54–56], and one can suppose that the growth of phytoplankton should be accelerated in local regions affected by small river plumes in Arctic conditions. From one point of view, these plumes bring water with high nutrient content that should accelerate productivity, but from another these turbid freshwater plumes can also shade available light, stratify the water column, and inhibit nutrient-rich deep water renewal [56]. There are other studies on the small river plumes in the Arctic [57], but we still need to expand our observations to understand their influence on the coastal biogeochemical regime.

4.4. Future Projections

The Arctic Ocean and the Svalbard archipelago are facing rapid changes due to global warming. One expects that the intrusion of warm and saline Atlantic water [24,58] will facilitate the melting of Svalbard glaciers [52]. In turn, runoff from glaciers and rivers will lead to estuarine circulation in the fjord [56]. Climate-change-driven increases in freshwater discharge should lead to increased suspended sediment loads, and the mobilization and transport of terrestrial carbon and nutrients from thawing and greening watersheds [27]. In this study, we show the difference in chemical regime near the discharge sources compared with marine parts of the fjord. In the last decades, there have been processes documented such as glacier mass loss, permafrost warming, increases in freshwater runoff, and changes in precipitation patterns [59–61]. Experiments on the influence of thawing permafrost on coastal seawater chemical properties also demonstrated the effect of nutrient inputs, ocean acidification, heavy metals, and pollutants [19]. The Arctic Ocean is surrounded by permafrost, which is being degraded at an increasing rate [15]. All these processes, intensifying under conditions of warming, could lead to significant consequences for all marine polar ecosystems.

Since these processes are expected to continue during this century, they will have consequences for the future biogeochemical regime and ecosystems in the coastal zones. Our studies demonstrate an enrichment with nutrients of the water originated or affected by the coastal discharge and glacial melting, which indicates potentially higher biological productivity there. Increasing temperature will lead to a longer melting period and therefore a larger volume of coastal water with higher productivity. Another negative consequence is increased oxygen depletion: in the coastal regions, oxygen will be consumed for oxidation of the increased amount of organic matter connected with higher biological productivity, and of the organic matter created by the permafrost thawing, as we showed with the permafrost melting experiment [61]. As we observe here, glacial water is characterized by smaller values of total inorganic carbon and alkalinity. The aragonite saturation value near the glacier was low (<1.5) in both winter and summer; with the glacier melting intensification, the saturation may drop below 1, with negative consequences for the ecosystem [19].

5. Conclusions

The seasonal variability of the biogeochemical characteristics of the water column in fjord systems is determined by the formation and destruction of stratification, continental runoff, and aquatic biota activity, and differs in the near-glacier region and the outer fjord.

The influence of the glacier can be detected from late winter (March) in terms of salinity, alkalinity, and silicate, with especially high concentrations ($>40 \mu\text{M}$), observed as local maxima at different depths and locations, potentially reflecting the patchy structure of the glacial plume formed by the upwelling of subglacial discharge.

Near-glacier regions can have potentially higher biological productivity due to the supply of nutrients from coastal and subglacial discharge water and the faster restoration of nutrients after the summer blooms (September) in the area. As follows from the Redfield ratio, nitrogen is the limiting element for photosynthesis, and nitrate values are low in the outer fjord and near the glacier.

River plumes can be detected at a distance of 1.5–2 km from the river mouth by the low alkalinity and high concentration of silicate.

Silicate appears to be the best parameter for detecting river water and glacial melt water. This is connected with high concentrations of this element in the bedrock.

The nutrients measured in the Arctic environmental media were minimal in the glacial region and in river and sea ice, with medium concentrations at the sea surface, deep seawater, and river water, and maximum concentrations in the bottom sediments.

These results are based on short arrays of observations, and we must highlight the necessity for new studies with a finer spatial resolution (first of all near the glacier) and more frequent sampling. More dedicated data are needed to better understand the ongoing processes and possible changes that could occur in the Arctic environment.

Author Contributions: Conceptualization, E.Y., M.P.; Data curation, E.Y., A.P. and P.M.; Formal analysis, M.P., A.P., P.M. and A.S.; Funding acquisition, E.Y.; Investigation, E.Y., M.P., A.P., P.M. and A.S.; Methodology, E.Y., M.P., A.P., P.M., A.S. and A.B.; Resources, E.Y., A.S.; Software, A.B.; Validation, E.Y., A.P., P.M. and A.B.; Visualization, E.Y., M.P., A.P. and A.B.; Writing—original draft, E.Y., M.P. and A.P.; Writing—review and editing, M.P., A.P. and A.S. All authors have read and agreed to the published version of the manuscript.

Funding: This research was funded by The Research Council of Norway: 227151 CARSIC; The Research Council of Norway: 283482 ICOTA; The Research Council of Norway: 315317 BEST-Siberian; Russian Science Foundation Grant 21-77-30001; The Research Council of Norway: 246752 POMPA.

Institutional Review Board Statement: Not applicable.

Informed Consent Statement: Not applicable.

Data Availability Statement: Not applicable.

Acknowledgments: Our research group would like to thank Gerd Irene Sigernes for the provision of a chemistry laboratory at the UNIS, Spitzbergen and our colleagues who participated in the studies: Ali Alyautdinov, Alisa Ilinskaya, Marit Norli, Svetlana Stepanova, Shamil Yakubov, and Elizaveta Protsenko.

Conflicts of Interest: The authors declare no conflict of interest.

Appendix A

Appendix A.1. Vertical Distributions of the Studied Parameters at the Sampled Stations

Appendix A.1.1. Winter expedition, February 2011

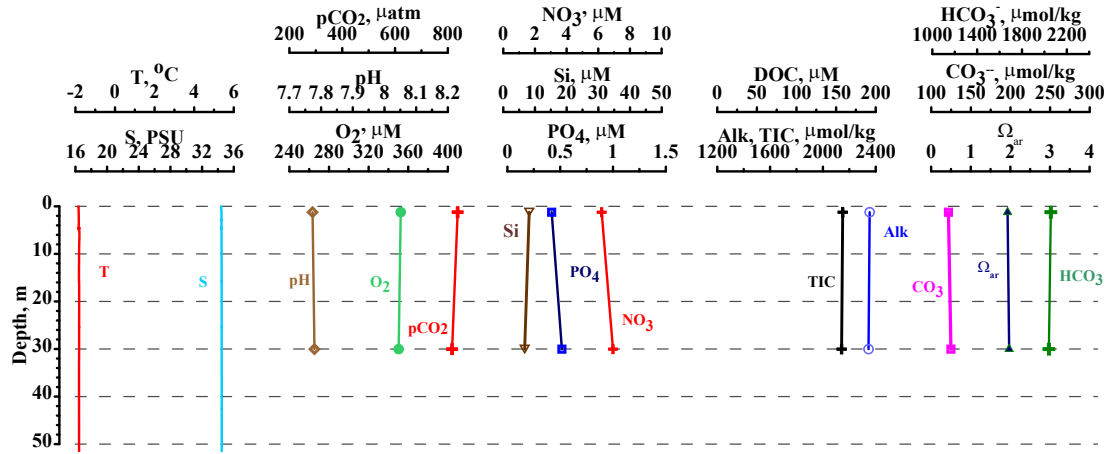


Figure A1. Vertical distribution of physical and chemical parameters at station T4 (19 February 2011).

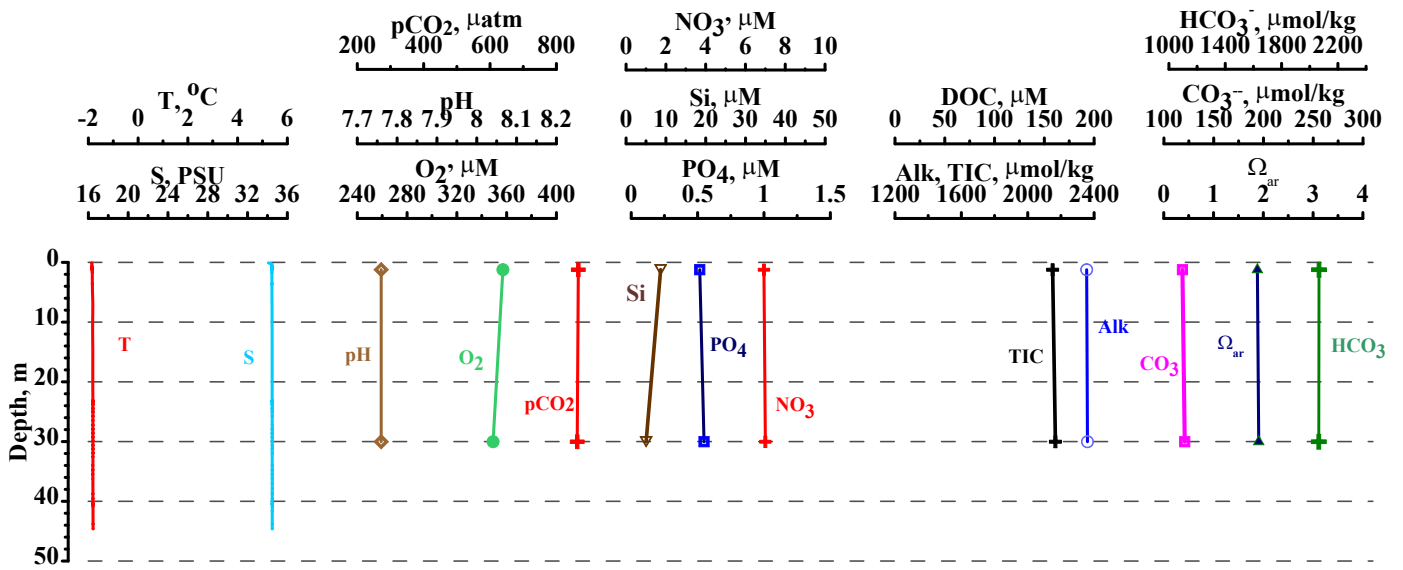


Figure A2. Vertical distribution of physical and chemical parameters at station T5 (19 February 2011).

Appendix A.1.2. Winter expedition, March 2014

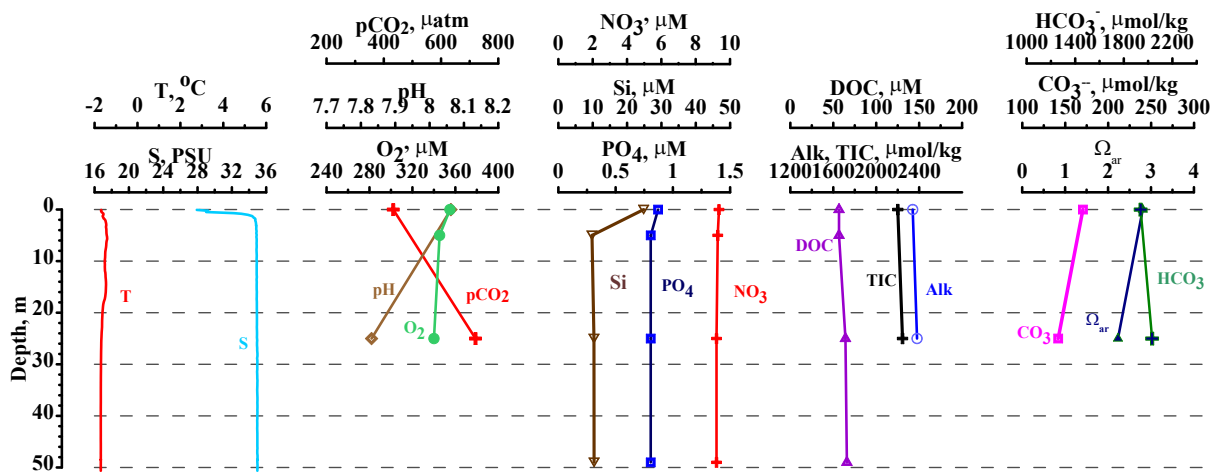


Figure A3. Vertical distribution of physical and chemical parameters at station TM1 (17 March 2014).

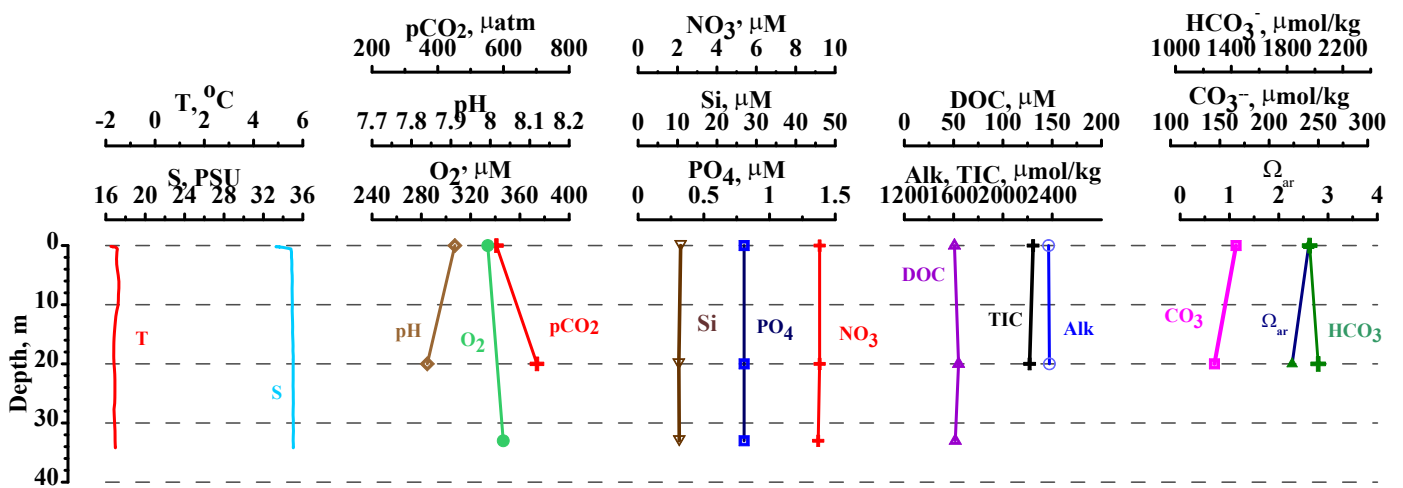


Figure A4. Vertical distribution of physical and chemical parameters at station TM2 (17 March 2014).

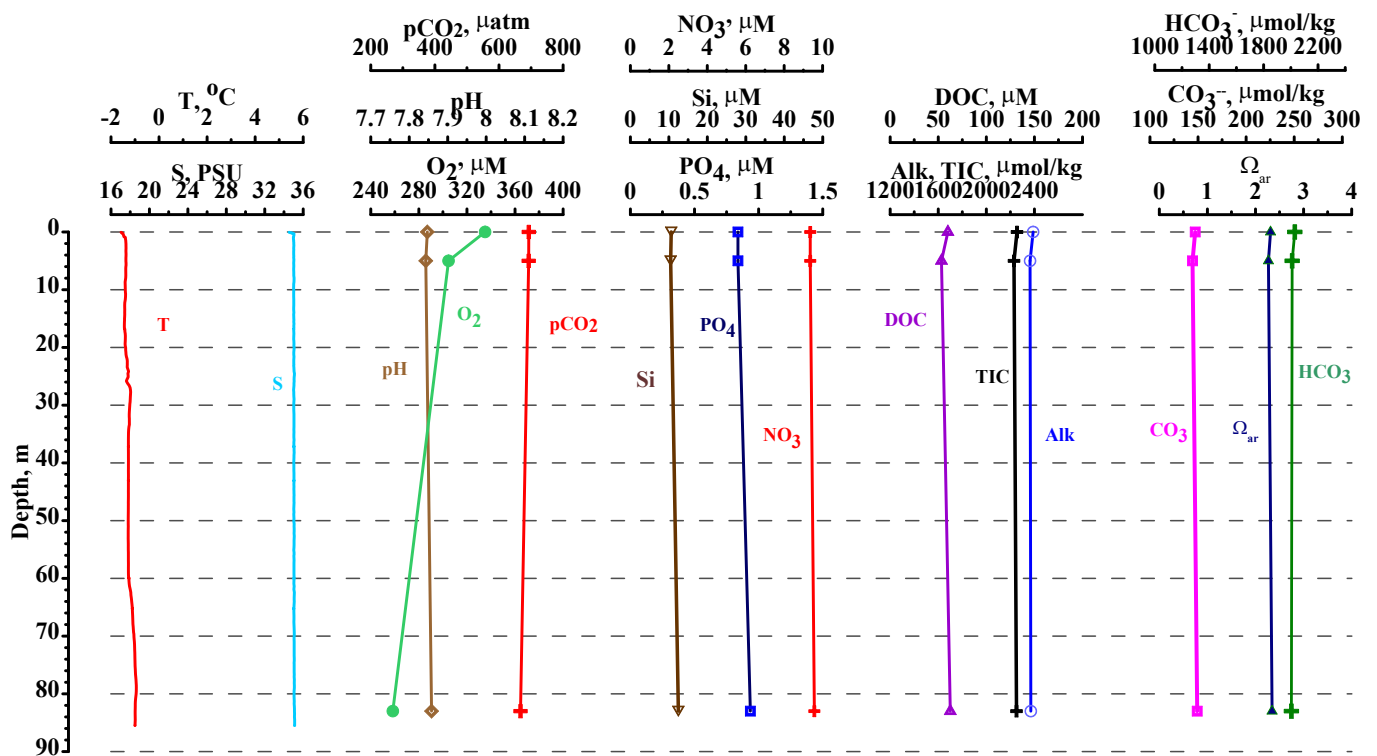


Figure A5. Vertical distribution of physical and chemical parameters at station TM4 (19 March 2014).

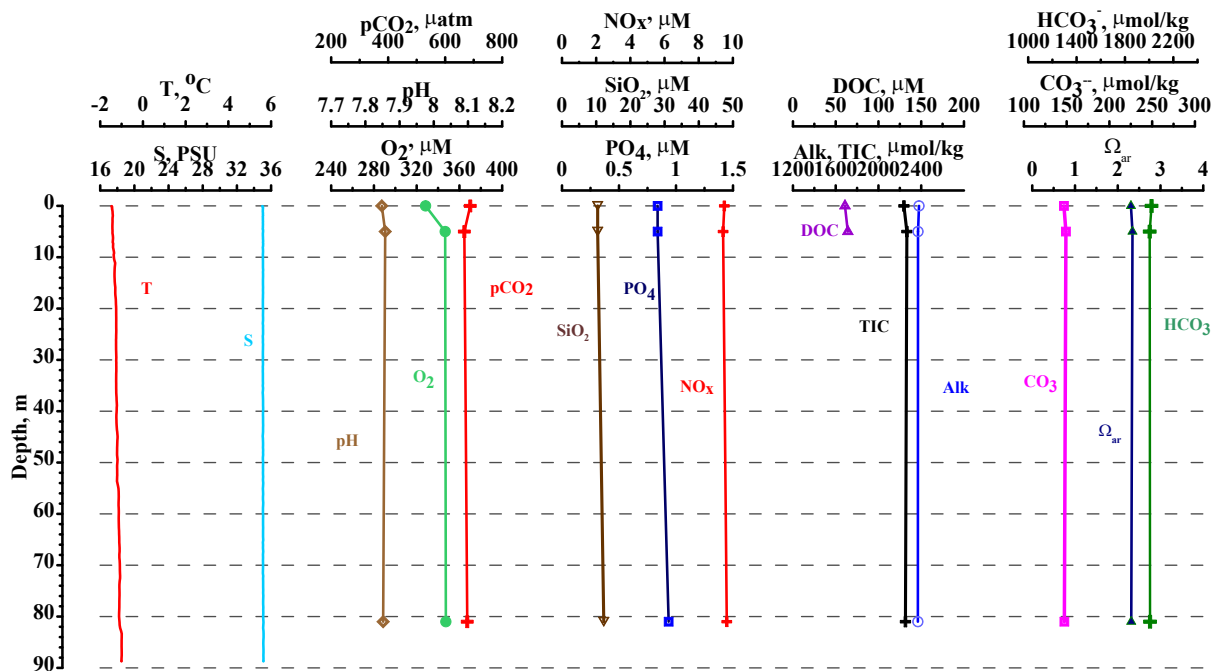


Figure A6. Vertical distribution of physical and chemical parameters at station TM5 (19 March 2014).

Appendix A.1.3. Summer expedition, June 2015

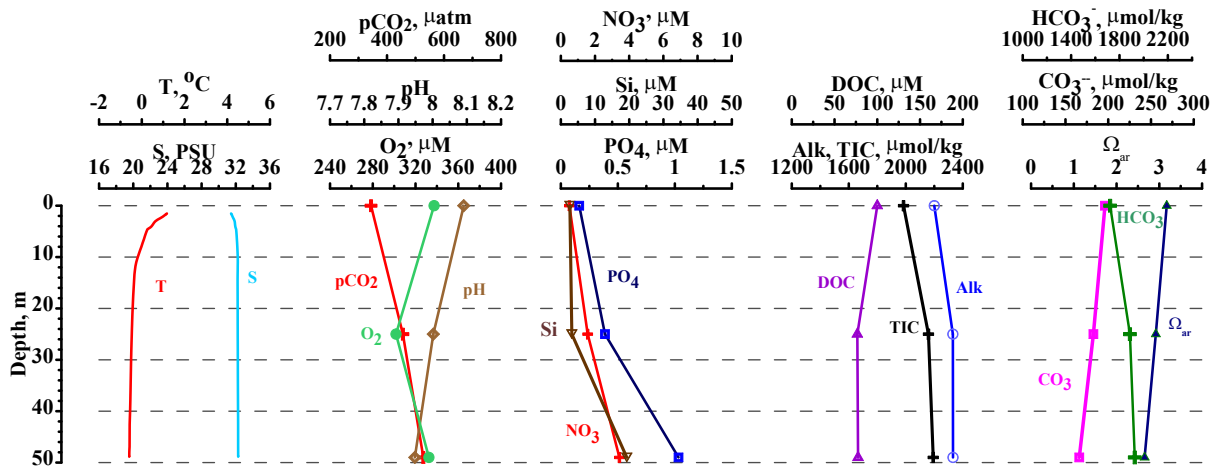


Figure A7. Vertical distribution of physical and chemical parameters at station TJ2 (17 June 2015).

Appendix A.1.4. Summer expedition, September 2011

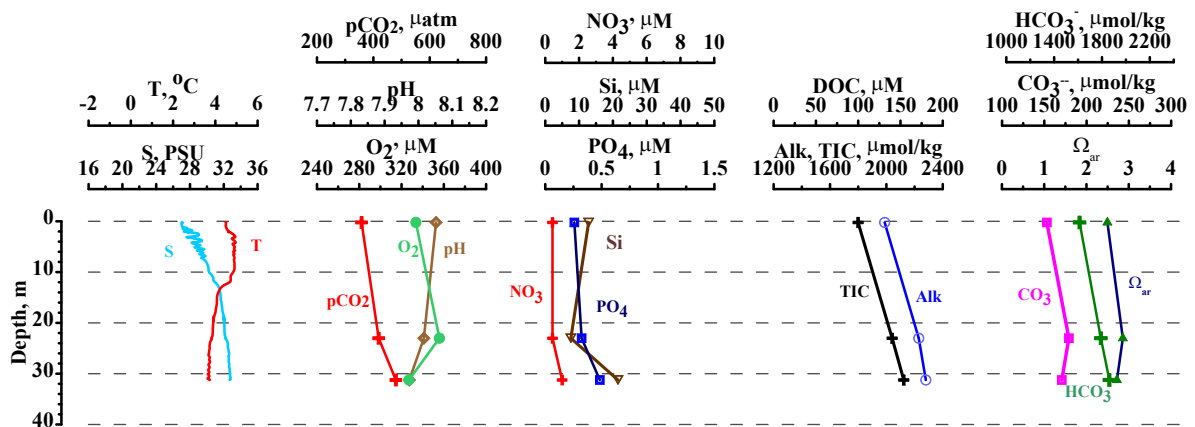


Figure A8. Vertical distribution of physical and chemical parameters at station TS2 (06 September 2011).

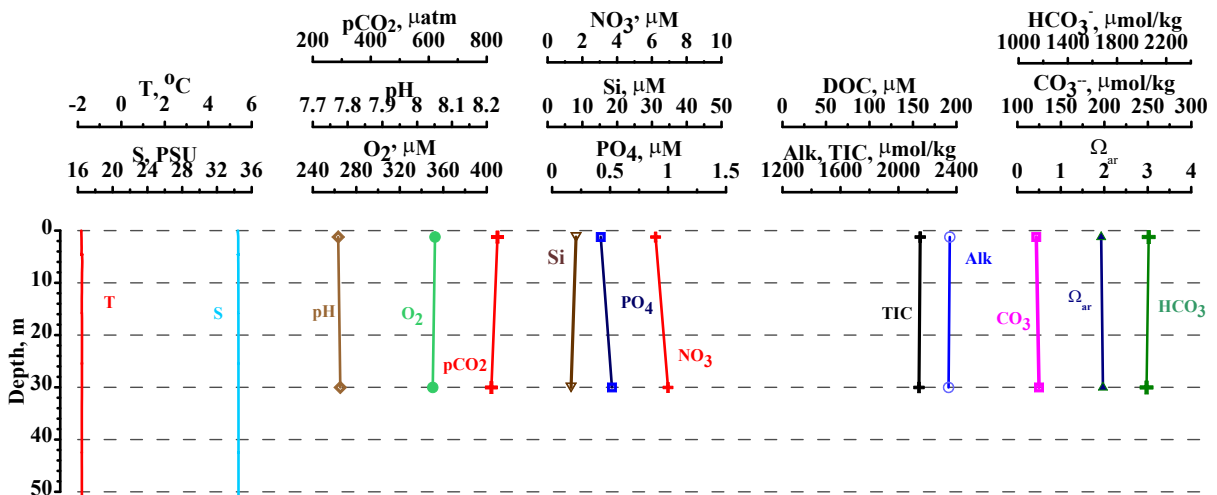


Figure A9. Vertical distribution of physical and chemical parameters at station TF4 (14 June 2017).

In the ice cores of station TM1, the nutrient concentration was 2–3 times lower than in the surface layer under the ice (A 1). The alkalinity was 4–5 times lower and DOC was a little lower in the ice core as well. In the ice core of station TM-2, all values were approximately half less than in the ice core on TM-1. It seems that brine flows faster through the ice away from the glacier.

Table A1. Data on the vertical structure of the ice cores on sites TM-1 and TM-2.

Site #	Layer cm	Temp. °C	Alk μM	PO_4 μM	Si μM	$\text{NO}_3 + \text{NO}_2$ μM	DIC μM	DOC μM	Hg Total ng/L	MeHg ng/L
TM-1										
	0–18	−3.23	503.7	0.26	12.5	2.2	383.33	59.17	0.8	0.01
	18–36	−1.67	374.1	0.23	9.7	1.5	286.67	65		
	36–52	−1.24	378.9	0.26	12.2	1.6	280	60.83		
TM-2										
	0–10	−3.85	259.1	0.13	4.4	0.8	154.17	31.67	0.7	0.01
	10–20	−2.11	338.5	0.16	4.6	1.2	234.17	100		
	20–30	−1.96	407.9	0.23	6.9	1.6	316.67	108.33		

During the summer expedition in 2017, bottom sediments were collected in Templefjord in front of the river, near the glacier, and in the river. In Adventifjord, samples of bottom sediments and permafrost were also collected near Longyearbean.

In general, the grain size composition was silty in bottom sediment samples with a lower particle size and sandy in permafrost and river sediments (A2, 3).

Table A2. Grain size composition of bottom sediments in Templefjord in front of the river (TG-1) near the glacier (TF-4), in permafrost (TG-8), and in riverine sediments (R) (June 2017).

Station	Psephite	Grain Size Composition %			Shepard Class
		Sand	Silt	Clay	
TG-1	0	29.54	30.53	39.94	Sand/silt/clay
TF-4	0	1.85	56.94	41.21	Clayey silt
TG-8	82.15	17.84	0	0.00	Sandy psephite
R	64.69	24.79	9.40	1.12	Sandy psephite

Table A3. Data on nutrient content in the pore water of bottom sediments in Templefjord in front of the river (TG-1) near the glacier (TF-4), in permafrost (TG-8), and in Longyearbean harbor (H) (June 2017).

Sample_ID	Depth	NH_4 (μM)	P-PO_4 (μM)	$\text{NO}_2 + \text{NO}_3$ (μM)	DOC (μM)	Si (μM)	TIC, μM	Alk, μM
TG-1	80	139	3.55	1.43	8318.07	199.36		
TF-4	51	0	1.29	17.13	5703.58	238.52		
TG-8	0	172	22.60	46.40	899.25	142.40	10.8	1.5
H		111	4.84	5.00	8301.42	206.48		

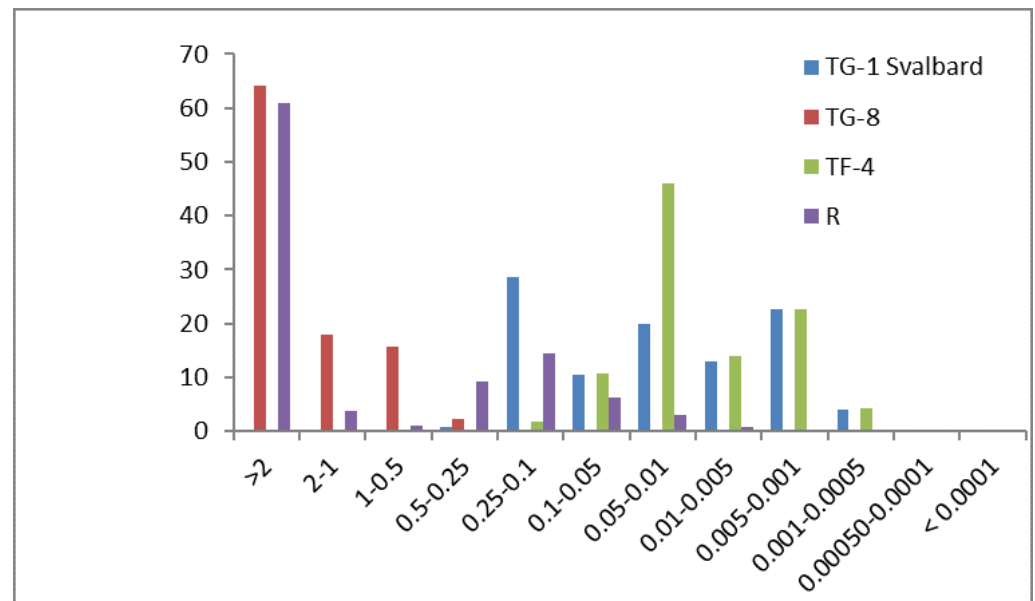


Figure A10. The distribution of grain size composition of bottom sediments in Templefjord in front of the river (TG-1), near the glacier (TF-4), in permafrost (TG-8), and in riverine sediments (R) (June 2017).

Table A4. Data on nutrient content in seawater ice (TGSi), snow (TGSN), freshwater ice (TGFI), and glacier ice (TGGI) in Templefjord (June 2017).

Sample_ID	Matrix	pH In Situ	P-PO ₄ (μM)	NO ₂ + NO ₃ (μM)	DOC (μM)	Si (μM)
TGSi	Seawater ice	6.54	0.45	2.00	8.33	3.56
TGSN	Snow	8.12	0.19	0.29	17.49	8.19
TGFI	Fresh water ice	8.12	0.10	0.21	10.82	2.85
TGGI	Glacier ice	7.53	0.03	0.21	18.32	1.28

Table A5. Data on carbon content in the bottom sediments in Templefjord in front of the river (TG-1) near the glacier (TF-4), in permafrost (TG-8), and in riverine sediments (R) (June 2017).

Parameter		Total Carbon (TC) %	Total Inorganic Carbon (TIC) %	Total Organic Carbon (TOC) %
Samples				
TG-1	12.06.2017	4.42	3.49	0.93
TF-4	14.06.2017	5.27	5.03	0.24
TG-8	14.06.2017	0.53	0.08	0.45
R	12.06.2017	8.76	9.20	<0.1

Table A6. Seasonal and interannual changes of nutrients in the surface layer, not affected by the river plume in the near-glacier region and the outer fjord.

Parameters/Expeditions	19 February 2011	17–19 March 2014	11–17 June 2017	17–18 June 2015	6 September 2011	
O ₂	glacier	353.1 ± 3.7	359.3 ± 27.8	392.4	357.4 ± 28.4	366.2
	outer fjord	350.3	331.7 ± 4.8	393.2	369.2	333.6
pH	glacier	7.75 ± 0.01	8.18 ± 0.02	8.46	8.39 ± 0.02	8.33
	outer fjord	7.76	8.2 ± 0.01	8.37	8.5	8.3
Alk	glacier	2352 ± 5	2353 ± 17	1475	1956 ± 346	1757
	outer fjord	2345	2384 ± 7	2238	2225	1988
PO ₄	glacier	0.49 ± 0.07	0.83 ± 0.04	0.16	0.18 ± 0.02	1.03
	outer fjord	0.55	0.84 ± 0.0	0.26	0.16	0.26
NO ₃	glacier	6.76 ± 0.49	9.24 ± 0.11	1.21	0.82 ± 0.45	1.29
	outer fjord	7.29	9.43 ± 0.1	0.14	0.14	0.43
Si	glacier	10.23 ± 3.12	15.31 ± 8.24	18.87	4.04 ± 1.97	46.93
	outer fjord	6.04	10.52 ± 0.13	3.1	2.64	12.82
TIC	glacier	2156 ± 10	2223 ± 22	1387	1763 ± 312	1592
	outer fjord	2166.67	2247 ± 12	2026	2010	1799
DOC	glacier		60.0 ± 11.2	75.8	133.3 ± 47.1	
	outer fjord		60.4 ± 0.6	80.8	100.0	
Ω _{ar}	glacier	1.31 ± 0.02	1.52 ± 0.06		1.8 ± 0.48	1.4
	outer fjord	1.35	1.61 ± 0.03		2.81	1.77

Table A7. Seasonal and interannual changes of nutrients in the bottom layer in the near glacier region and the outer fjord.

Parameters/Expeditions	19 February 2011	17–19 March 2014	11–17 June 2017	17–18 June 2015	6 September 2011	
O ₂	glacier	347.8 ± 3.4	348.1 ± 9.0	323.05	328.2 ± 6.1	320.8
	outer fjord	354.7	302.8 ± 62.9	360.2 ± 36.8	341.6	327.0
pH	glacier	7.74 ± 0.01	8.21 ± 0.04	8.24	8.21 ± 0.07	8.24
	outer fjord	7.76	8.21 ± 0.0	8.32 ± 0.11	8.34	8.22
Alk	glacier	2344 ± 16	2374. ± 8.	2323	2361 ± 42	2279.
	outer fjord	2343	2369. ± 0.9	2302. ± 22.7	2356.1	2279.9
PO ₄	glacier	0.53 ± 0.02	1.1 ± 0.58	0.84	0.94 ± 0.14	0.55
	outer fjord	0.52	0.94 ± 0.0	0.5 ± 0.27	0.52	0.48
NO ₃	glacier	7.0 ± 0.07	9.37 ± 0.37	7.49	6.36 ± 4.14	1.14
	outer fjord	6.86	9.61 ± 0.05	2.19 ± 2.94	4.14	1.0
Si	glacier	6.35 ± 1.16	20.92 ± 21.05	8.9	14.34 ± 7.0	23.96
	outer fjord	5.96	12.34 ± 0.18	3.99 ± 2.77	5.46	21.5
TIC	glacier	2156 ± 13	2246 ± 1.8	2203.	2216 ± 34	2144
	outer fjord	2175	2252 ± 2	1809 ± 500.	2211	2123
DOC	glacier		58.8 ± 7.3	74.1	101.3 ± 33.6	
	outer fjord		62.5	53.3 ± 46.3	108.3	
Ω _{ar}	glacier	1.3 ± 0.04	1.5 ± 0.34		1.58 ± 0.21	2.1
	outer fjord	1.34	1.66 ± 0.0		2.06	1.91

Table A8. The list of stations, locations, studied parameters and environmental media in different expeditions performed in this study.

Date	St.№	Latitude	Longitude	Parameters							Media						
				T and S	Nutrients	Carbonate System	Trace Metals	Seawater	River Water	Sea ice Cores	Drifting Sea ice	River Ice	Glacial Ice	Snow	Sea sediments	River Bed sediments	Abrasive Cliff
19 February 2011	T4	78.45325	17.34700	X	X	X		X									
19 February 2011	T5	78.44022	17.40878	X	X	X		X									
19 February 2011	T1	78.44415	17.36887	X	X	X		X									
19 February 2011	T7	78.39082	16.87540	X	X	X		X									
06 September 2011	TS1	78.44392	17.36030	X	X	X		X									
06 September 2011	TS2	78.42430	17.18807	X	X	X		X									
17/03/2014	TM1	78.44622	17.37732	X	X	X		X		X							
17 March 2014	TM2	78.42933	17.28628	X	X	X		X		X							
18 March 2014	TM3	78.43598	17.33338	X	X	X		X		X							
19 March 2014	TM4	78.37632	16.84408	X	X	X		X		X							
19 March 2014	TM5	78.37537	16.78647	X	X	X		X									
17 June 2015	TJ1	78.43347	17.23838	X	X	X	X	X									
17 June 2015	TJ2	78.43752	17.17472	X	X	X	X	X									
17 June 2015	TJ3	78.40668	17.08752	X	X	X	X	X									
12 June 2017	TG1	78.40668	17.09198	X	X	X	X	X									X
14 June 2017	TF4	78.43581	17.29440	X	X	X	X	X									X
13 June 2017	R	78.42172	17.05333	X	X		X		X			X					X
12 June 2017	TGSI	78.42172	17.05333	X	X		X			X							
12 June 2017	TGSN	78.42172	17.05333	X	X		X							X			
12 June 2017	TGFI	78.42172	17.0533	X	X		X					X					
12 June 2017	TGGI	78.43483	17.29747	X	X		X						X				
13 June 2017	H	78.24030	15.55513				X										X

References

1. IASC. *2020 State of Arctic Science Report*; The International Arctic Science Committee: Akureyri, Iceland, 2020.
2. IPCC. *Climate Change 2014: Synthesis Report. Contribution of Working Groups I, II and III to the Fifth*; IPCC: Geneva, Switzerland, 2014.
3. Overpeck, J.; Hughen, K.; Hardy, D.; Bradley, R.; Case, R.; Douglas, M.; Finney, B.; Gajewski, K.; Jacoby, G.; Jennings, A.; et al. Arctic environmental change of the last four centuries. *Science* **1997**, *278*, 1251–1256. [[CrossRef](#)]
4. Overland, J.E.; Wang, M.; Salo, S. The recent Arctic warm period. *Tellus Ser. A Dyn. Meteorol. Oceanogr.* **2008**, *60 A*, 589–597. [[CrossRef](#)]
5. Stroeve, J.; Serreze, M.; Drobot, S.; Gearheard, S.; Holland, M.; Maslanik, J.; Meier, W.; Scambos, T. Arctic sea ice extent plummets in 2007. *Eos* **2008**, *89*, 13–14. [[CrossRef](#)]
6. Min, S.K.; Zhang, X.; Zwiers, F. Human-induced Arctic moistening. *Science* **2008**, *320*, 518–520. [[CrossRef](#)] [[PubMed](#)]
7. McClelland, J.W.; Déry, S.J.; Peterson, B.J.; Holmes, R.M.; Wood, E.F. A pan-arctic evaluation of changes in river discharge during the latter half of the 20th century. *Geophys. Res. Lett.* **2006**, *33*, L06715. [[CrossRef](#)]

8. Bellerby, R.G.J.; Olsen, A.; Furevik, T.; Anderson, L.G. Response of the surface ocean CO₂ system in the Nordic seas and northern North Atlantic to climate change. In *The Nordic Seas: An Integrated Perspective: Oceanography, Climatology, Biogeochemistry, and Modeling*; American Geophysical Union: Washington, DC, USA, 2005; Volume 158, pp. 189–197. ISBN 978-0-87590-423-8.
9. AMAP. *Snow, Water, Ice and Permafrost in the Arctic (SWIPA)*; Arctic Monitoring and Assessment Programme: Oslo, Norway, 2017.
10. Hoegh-Guldberg, O.; Mumby, P.J.; Hooten, A.J.; Steneck, R.S.; Greenfield, P.; Gomez, E.; Harvell, C.D.; Sale, P.F.; Edwards, A.J.; Caldeira, K.; et al. Coral reefs under rapid climate change and ocean acidification. *Science* **2007**, *318*, 1737–1742. [[CrossRef](#)] [[PubMed](#)]
11. Steinacher, M.; Joos, F.; Frölicher, T.L.; Plattner, G.K.; Doney, S.C. Imminent ocean acidification in the Arctic projected with the NCAR global coupled carbon cycle-climate model. *Biogeosciences* **2009**, *6*, 515–533. [[CrossRef](#)]
12. Semiletov, I.; Pipko, I.; Gustafsson, Ö.; Anderson, L.G.; Sergienko, V.; Pugach, S.; Dudarev, O.; Charkin, A.; Gukov, A.; Bröder, L.; et al. Acidification of East Siberian Arctic Shelf waters through addition of freshwater and terrestrial carbon. *Nat. Geosci.* **2016**, *9*, 361–365. [[CrossRef](#)]
13. Bellerby, R.G.J.; Schulz, K.G.; Riebesell, U.; Neill, C.; Nondal, G.; Heegaard, E.; Johannessen, T.; Brown, K.R. Marine ecosystem community carbon and nutrient uptake stoichiometry under varying ocean acidification during the PeECE III experiment. *Biogeosciences* **2008**, *5*, 1517–1527. [[CrossRef](#)]
14. Semiletov, I.P.; Pipko, I.I.; Repina, I.; Shakhova, N.E. Carbonate chemistry dynamics and carbon dioxide fluxes across the atmosphere—ice—water interfaces in the Arctic Ocean: Pacific sector of the Arctic. *J. Mar. Syst.* **2007**, *66*, 204–226. [[CrossRef](#)]
15. Semiletov, I.P.; Shakhova, N.E.; Sergienko, V.I. On carbon transport and fate in the East Siberian Arctic land—shelf—atmosphere system. *Environ. Res. Lett.* **2012**, *7*, 015201. [[CrossRef](#)]
16. Shakhova, N.; Semiletov, I.; Chuvilin, E. Understanding the permafrost–hydrate system and associated methane releases in the east siberian arctic shelf. *Geosciences* **2019**, *9*, 251. [[CrossRef](#)]
17. Tesi, T.; Muschitiello, F.; Smittenberg, R.H.; Jakobsson, M.; Vonk, J.E.; Hill, P.; Andersson, A.; Kirchner, N.; Noormets, R.; Dudarev, O.; et al. Massive remobilization of permafrost carbon during post-glacial warming. *Nat. Commun.* **2016**, *7*, 13653. [[CrossRef](#)] [[PubMed](#)]
18. Vonk, J.E.; Sánchez-García, L.; van Dongen, B.E.; Alling, V.; Kosmach, D.; Charkin, A.; Semiletov, I.P.; Dudarev, O.V.; Shakhova, N.; Roos, P.; et al. Activation of old carbon by erosion of coastal and subsea permafrost in Arctic Siberia. *Nature* **2012**, *489*, 137–140. [[CrossRef](#)]
19. Pogojeva, M.; Yakushev, E.; Ilinskaya, A.; Polukhin, A.; Braaten, H.; Kristiansen, T. Experimental study of the influence of thawing permafrost on the chemical properties of sea water. *Russ. J. Earth Sci.* **2018**, *18*, 2–7. [[CrossRef](#)]
20. Hagen, J.O.; Liestøl, O.; Roland, E.; Jørgensen, T. *Glacier atlas of Svalbard and Jan Mayen*; Norsk Polarinstitutt Meddelelser: Oslo, Norway, 1993; p. 144.
21. Kohler, J.; James, T.D.; Murray, T.; Nuth, C.; Brandt, O.; Barrand, N.E.; Aas, H.F.; Luckman, A. Acceleration in thinning rate on west-ern Svalbard glaciers. *Geophys. Res. Lett.* **2007**, *34*. [[CrossRef](#)]
22. Nuth, C.; Moholdt, G.; Kohler, J.; Hagen, J.O.; Kääb, A. Svalbard glacier elevation changes and contribution to sea level rise. *J. Geophys. Res.* **2010**, *115*. [[CrossRef](#)]
23. Moholdt, G.; Hagen, J.O.; Eiken, T.; Schuler, T.V. Geometric changes and mass balance of the Austfonna ice cap, Svalbard. *Cryosphere* **2010**, *4*, 21–34. [[CrossRef](#)]
24. Polyakov, I.V.; Pnyushkov, A.V.; Alkire, M.B.; Ashik, I.M.; Baumann, T.M.; Carmack, E.C.; Goszczko, I.; Guthrie, J.; Ivanov, V.V.; Kanzow, T.; et al. Greater role for Atlantic inflows on sea-ice loss in the Eurasian Basin of the Arctic Ocean. *Science* **2017**, *356*, 285–291. [[CrossRef](#)]
25. Fransson, A.; Chierici, M.; Nomura, D.; Granskog, M.A.; Kristiansen, S.; Martma, T.; Nehrke, G. Effect of glacial drainage water on the CO₂ system and ocean acidification state in an Arctic tidewater-glacier fjord during two contrasting years. *J. Geophys. Res. C Ocean.* **2015**, *120*, 2413–2429. [[CrossRef](#)]
26. Nilsen, F.; Cottier, F.R.; Skogseth, R.; Mattson, S. Fjord–shelf exchanges controlled by ice and brine production: The interannual variation of Atlantic Water in Isfjorden, Svalbard. *Cont. Shelf Res.* **2008**, *28*, 1838–1853. [[CrossRef](#)]
27. McGovern, M.; Pavlov, A.K.; Deininger, A.; Granskog, M.A.; Leu, E.; Søreide, J.E.; Poste, A.E. Terrestrial Inputs Drive Seasonality in Organic Matter and Nutrient Biogeochemistry in a High Arctic Fjord System (Isfjorden, Svalbard). *Front. Mar. Sci.* **2020**, *7*, 747. [[CrossRef](#)]
28. Yakushev, E.V.; Makkaveev, P.N.; Polukhin, A.A.; Protsenko, E.A.; Stepanova, S.V.; Khlebopashev, P.V.; Yakubov, S.K.; Staalstrøm, A.; Norli, M. Hydrochemical studies in coastal waters of the Spitsbergen Archipelago in 2014–2015. *Oceanology* **2016**, *56*, 763. [[CrossRef](#)]
29. Polukhin, A.; Yakushev, E.; Makkaveev, P.; Protsenko, E.; Yakubov, S.; Stepanova, S.; Khlebopashev, P.; Norli, M.; Braaten, H.; Introduction, I. Influence of melting glaciers on hydrochemical structure of coastal ecosystem of Western Spitsbergen. In Proceedings of the XXVI International Shore Conference "Managing Risks to Coastal Regions and Communities in a Changing World", St. Petersburg, Russia, 22–27 August 2016.
30. Welty, E.Z.; Bartholomäus, T.C.; Liu, Y.; Riikilä, T.I.; Zwinger, T.; Timonen, J.; Moore, J.C.; Åström, J.A.; Vallot, D.; Schäfer, M.; et al. Termini of calving glaciers as self-organised critical systems. *Nat. Geosci.* **2014**, *7*, 874–878. [[CrossRef](#)]
31. Marchenko, A.; Morozov, E.; Muzylev, S. Measurements of sea-ice flexural stiffness by pressure characteristics of flexural-gravity waves. *Ann. Glaciol.* **2013**, *54*, 51–60. [[CrossRef](#)]

32. Hansen, H.P.; Koroleff, F. Determination of nutrients. In *Methods of Seawater Analysis, 3rd Completely Revised and Extended Edition*; Wiley: Hoboken, NJ, USA, 2007; pp. 159–228. ISBN 9783527613984.
33. Dickson, A.G.; Goyet, C. Handbook of methods for the analysis of the various parameters of the carbon dioxide system in sea water. *DOE Handb.* **1992**, *1994*, 22.
34. Dickson, A.G.; Sabine, C.L.; Christian, J.R. *Guide to Best Practices for Ocean CO₂ Measurements*; PICES Special Publication 3, IOCCP Report No. 8; North Pacific Marine Science Organization: Sidney, BC, Canada, 2007.
35. Yakushev, E.; Sørensen, K. On seasonal changes of the carbonate system in the Barents Sea Observations and modeling.pdf. *Mar. Biol. Res.* **2013**, *822–830*. [[CrossRef](#)]
36. Lewis, E.; Wallace, D. *Program developed for CO₂ system calculations, Carbon Dioxide Information Analysis Center, managed by Lockheed Martin Energy Research Corporation for the US Department of Energy*; NOAA: Asheville, NC, USA, 1998.
37. Gundersen, C.B.; Kaste, Ø.; Sample, J.; Fredrik, H.; Braaten, V.; Selvik, J.R.; Hjermann, D.Ø.; Norling, M.D.; Guerrero Calidonio, J.-L. *The Norwegian River Monitoring Programme—Water Quality Status and Trends 2017*; Norwegian Institute for Water Research: Oslo, Norway, 2018.
38. Mintrop, L.; Pérez, F.F.; González-Dávila, M.; Santana-Casiano, J.M.; Körtzinger, A. Alkalinity determination by potentiometry: Intercalibration using three different methods. *Ciencias Mar.* **2000**, *26*, 23–37. [[CrossRef](#)]
39. Van Heuven, S.; Pierrot, D.; Rae, J.W.B.; Lewis, E.; Wallace, D.W.R. *MATLAB Program Developed for CO₂ System Calculations*; Carbon Dioxide Information Analysis Center Oak Ridge National Laboratory, U.S. Dept of Energy: Oak Ridge, TN, USA, 2011. [[CrossRef](#)]
40. Chierici, M.; Fransson, A. Calcium carbonate saturation in the surface water of the Arctic Ocean: Undersaturation in freshwater influenced shelves. *Biogeosciences* **2009**, *6*, 2421–2431. [[CrossRef](#)]
41. Flink, A.E.; Noormets, R.; Kirchner, N.; Benn, D.I.; Luckman, A.; Lovell, H. The evolution of a submarine landform record following recent and multiple surges of Tunabreen glacier, Svalbard. *Quat. Sci. Rev.* **2015**, *37–50*. [[CrossRef](#)]
42. Canfield, D.E.; Kristensen, E.; Thamdrup, B. Aquatic geomicrobiology. *Adv. Mar. Biol.* **2005**, *48*, 1–599. [[CrossRef](#)]
43. Yakushev, E.V.; Protsenko, E.A.; Bruggeman, J.; Wallhead, P.; Pakhomova, S.V.; Yakubov, S.K.; Bellerby, R.G.J.; Couture, R.-M. Bottom RedOx Model (BROM v.1.1): A coupled benthic-pelagic model for simulation of water and sediment biogeochemistry. *Geosci. Model Dev.* **2017**, *10*, 453–482. [[CrossRef](#)]
44. Marchenko, A.; Shestov, A.; Karulin, E.; Morozov, E.; Karulina, M.; Bogorodsky, P.; Muzylev, S.; Onishchenko, D.; Makshtas, A. Field studies of sea water and ice properties in Svalbard fjords. In *Proceedings of the International Conference on Port and Ocean Engineering under Arctic Conditions*, Montreal, QC, Canada, 10–14 July 2011; pp. 120–132.
45. Chierici, M.; Vernet, M.; Fransson, A.; Børsheim, K.Y. Net community production and carbon exchange from winter to summer in the Atlantic water inflow to the Arctic Ocean. *Front. Mar. Sci.* **2019**, *6*, 528. [[CrossRef](#)]
46. Halbach, L.; Vihtakari, M.; Duarte, P.; Everett, A.; Granskog, M.A.; Hop, H.; Kauko, H.M.; Kristiansen, S.; Myhre, P.I.; Pavlov, A.K.; et al. Tidewater glaciers and bedrock characteristics control the phytoplankton growth environment in an Arctic fjord. *Front. Mar. Sci.* **2019**, *6*, 254. [[CrossRef](#)]
47. Meire, L.; Mortensen, J.; Rysgaard, S.; Bendtsen, J.; Boone, W.; Meire, P.; Meysman, F.J.R. Spring bloom dynamics in a subarctic fjord influenced by tidewater outlet glaciers (Godthåbsfjord, SW Greenland). *J. Geophys. Res. Biogeosci.* **2016**, *121*, 1581–1592. [[CrossRef](#)]
48. Hopwood, M.J.; Carroll, D.; Dunse, T.; Hodson, A.; Holding, J.M.; Iriarte, J.L.; Ribeiro, S.; Achterberg, E.P.; Cantoni, C.; Carlson, D.F.; et al. Review article: How does glacier discharge affect marine biogeochemistry and primary production in the Arctic? *Cryosphere* **2020**, *14*, 1347–1383. [[CrossRef](#)]
49. Reiner Vonnahme, T.; Persson, E.; Dietrich, U.; Hejdukova, E.; Dybwad, C.; Elster, J.; Chierici, M.; Gradinger, R. Early spring subglacial discharge plumes fuel under-ice primary production at a Svalbard tidewater glacier. *Cryosphere* **2021**, *15*, 2083–2107. [[CrossRef](#)]
50. Lydersen, C.; Assmy, P.; Falk-Petersen, S.; Kohler, J.; Kovacs, K.M.; Reigstad, M.; Steen, H.; Strøm, H.; Sundfjord, A.; Varpe, Ø.; et al. The importance of tidewater glaciers for marine mammals and seabirds in Svalbard. *J. Mar. Syst.* **2014**, *129*, 452–471. [[CrossRef](#)]
51. Hagen, J.O.; Kohler, J.; Melvold, K.; Winther, J. Glaciers in Svalbard: Mass balance, runoff and freshwater flux. *Polar Res.* **2003**, *22*, 145–159. [[CrossRef](#)]
52. Luckmann, A.; Benn, D.I.; Cottier, F.; Bevan, S.; Nilsen, F.; Inall, M. Calving rates at tidewater glaciers vary strongly with ocean temperature. *Nat. Comm.* **2015**, *6*, 1–7. [[CrossRef](#)]
53. Makkaveev, P.N.; Polukhin, A.A.; Khlebopashev, P.V. The surface runoff of nutrients from the coasts of Blagopoluchiya bay of the Novaya Zemlya Archipelago. *Oceanology* **2013**, *53*, 539–546. [[CrossRef](#)]
54. Gaston, T.F.; Schlacher, T.A.; Connolly, R.M. Flood discharges of a small river into open coastal waters: Plume traits and material fate. *Estuar. Coast. Shelf Sci.* **2006**, *69*, 4–9. [[CrossRef](#)]
55. Zavialov, P.O.; Makkaveev, P.N.; Kononov, B.V.; Osadchiv, A.A.; Khlebopashev, P.V.; Pelevin, V.V.; Grabovskiy, A.B.; Izhitskiy, A.S.; Goncharenko, I.V.; Soloviev, D.M.; et al. Hydrophysical and hydrochemical characteristics of the sea areas adjacent to the estuaries of small rivers if the Russian coast of the Black Sea. *Oceanology* **2014**, *265–280*. [[CrossRef](#)]

56. Torsvik, T.; Albretsen, J.; Sundfjord, A.; Kohler, J.; Sandvik, A.D.; Skarghamar, J.; Lindbäck, K.; Everett, A. Impact of tidewater glacier retreat on the fjord system: Modeling present and future circulation in Kongsfjorden, Svalbard. *Estuar. Coast. Shelf Sci.* **2019**, *220*, 152–165. [[CrossRef](#)]
57. Błaszczak, M.; Ignatiuk, D.; Uszczyk, A.; Cielecka-Nowak, K.; Grabiec, M.; Jania, J.A.; Moskalik, M.; Walczowski, W. Freshwater input to the Arctic fjord Hornsund (Svalbard). *Polar Res.* **2019**, *38*, 3506. [[CrossRef](#)]
58. Fraser, N.J.; Skogseth, R.; Nilsen, F.; Inall, M.E. Circulation and exchange in a broad Arctic fjord using glider-based observations. *Polar Res.* **2018**, *37*. [[CrossRef](#)]
59. Adakudlu, M.; Andresen, J.; Bakke, J.; Beldring, S.; Benestad, R.; Bilt, W.; Bogen, J.; Borstad, C.; Breili, K.; Breivik, Ø.; et al. *Climate in Svalbard 2100—A Knowledge Base for Climate Adaptation*; Norwegian Environment Agency: Trondheim, Norway, 2019.
60. Van Pelt, W.J.J.; Pohjola, V.A.; Reijmer, C.H. The changing impact of snow conditions and refreezing on the mass balance of an idealized Svalbard Glacier. *Front. Earth Sci.* **2019**. [[CrossRef](#)]
61. Pogojeva, M.P.; Yakushev, E.V.; Petrov, I.N.; Yaeski, E.A. Experimental study of the permafrost thawing effect on the content of nutrients and heavy metals in seawater during abrasion destruction of the Arctic coast. *Arct. Ecol. Econ.* **2021**, *11*, 67–75. [[CrossRef](#)]